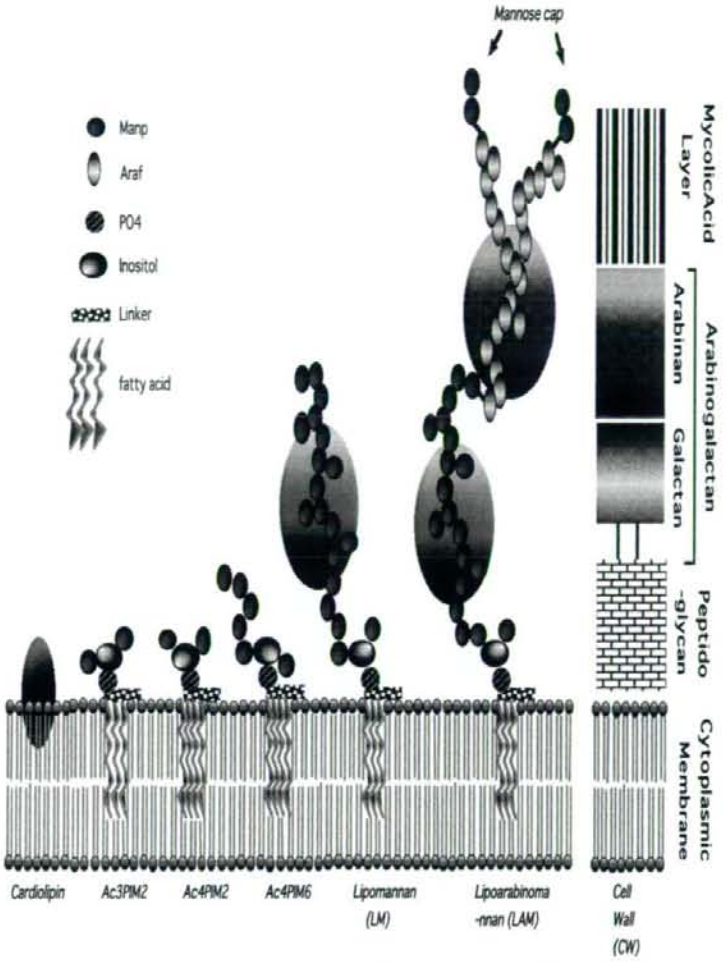

Fig. 1. Schematic structure of the mycobacterial cell envelopes. The individual compartment was shown to be a cytoplasmic membrane, peptidoglycan layer, arabinogalactan and mycolic acid layer (right side). The structures of the major lipid and lipoglycan molecules from BCG Tokyo-172 are shown; cardiolipin, Ac3PIM2, Ac4PIM2, Ac4PIM6, LM and LAM.

decade. LAM is a complex lipoglycan composed of D-mannan and D-arabinan attached to a PI moiety that anchors to the cytoplasmic membrane in the mycobacterial cell envelope (13). Although fatty acyl moiety is consistent among mycobacteria, the carbohydrate chain structure of LAM differs greatly according to the mycobacterial species, such as LAM with mannose caps (ManLAM), AraLAM and PILAM. However, the relationship between the molecular structure and immunomodulating activity of LAM has not yet been fully established especially in human immunocompetent systems.

Dendritic cells (DCs) play a crucial role in the induction of cellular immunity against intracellular pathogens including mycobacteria (14–16). Human or murine myeloid DC infected with *M. tuberculosis* or *M. bovis* BCG induced the maturation with an increased IL-12 production (17, 18) and induced a potent anti-tuberculous immunity against experimental tuberculosis in mice (19). A T_h1 cytokine IFN-γ has been identified as a key cytokine controlling mycobacterial infections (20–23). Patients defective in genes for IFN-γ or the IFN-γR are prone to serious mycobacterial infections (24). Therefore, IFN-γ plays a crucial role in anti-mycobacterial immunity. ManLAM, which is produced by slow-growing mycobacteria including *M. bovis* BCG, which has been reported to exert an immunosuppressive effect (25–27) and contributes to the persistence of slow-growing mycobacteria in humans. In contrast, LAM having phospho-myo-inositol units and LAM without capping are called PILAM and are produced from fast-growing mycobacteria. PILAM produces

a variety of pro-inflammatory cytokines through the activation of Toll-like receptor 2 (TLR2) (28–30). LM was shown to activate the macrophages in a TLR2-dependent and TLR4- and TLR6-independent manner (31–33). The balance of ManLAM/LM could thus be a parameter influencing the net immune responses against mycobacteria (34). Many investigators have reported that LAM/LM molecules induced type-I responses accompanied with the enhanced production of inflammatory cytokines, such as tumor necrosis factor α (TNFα) and IL-12 in DCs, and increased CD1 molecules on antigen-presenting cells (APCs). However, the regulation of the T_h1/T_h2 balance in the human immune system with PBMC induced by LAM/LM has not yet been reported.

In the present study, purified ManLAM/LM molecules from *M. bovis* BCG Tokyo-172 were structurally and functionally characterized, and the effect of LAM/LM on T_h1/T_h2 differentiation was assessed using an established human T_h1/T_h2 differentiation culture system. As a result, two distinct regulatory pathways were identified in which mycobacterial LAM/LM controls the balance of T_h1/T_h2 directly or indirectly via APCs.

Methods

Bacterial strain and growth conditions

Mycobacterium bovis BCG Tokyo-172 (ATCC 35737) was grown as a surface culture at 37°C in Sauton medium for 8 days. The bacterial culture was harvested by centrifugation after autoclaving at 121°C for 15 min.

Isolation and purification of LAM/LM, phosphatidylinositol dimannoside, hexamannoside and cardiolipin

Lipids were extracted with chloroform–methanol (2:1, by volume) and the crude lipids were separated by the solvent fractionation method (35). The PIMs [phosphatidylinositol dimannoside (PIM2) and hexamannoside (PIM6)] and cardiolipin were isolated from the chloroform-soluble fraction by thin-layer chromatography on a silica gel (Uniplate and Analtech) with the solvent system of chloroform–methanol–water (65:25:4, by volume). For purification of LAM/LM, the cells were re-suspended in deionized water and were passed three times through a French pressure cell (5501-MF, OHTAKE WORKS, Tokyo, Japan) at a pressure of 180 Mpa and disrupted. The unbroken cells were removed by centrifugation twice at 6760 × *g* for 20 min at 25°C. The broken cells (crude CW fraction) were separated from the supernatant by ultracentrifugation at 18 000 × *g* for 1 h at 25°C, and the supernatant containing lipoglycan was lyophilized. Contaminating glucans, proteins, DNA and RNA were removed by enzymatic degradation using α-amylase, trypsin, DNase 1 and RNase treatments followed by dialysis. An equal volume of 90% phenol was then added to the water containing lipoglycans, and the mixture was incubated with shaking at 68°C for 1 h. After separation of the aqueous phase from the phenol layer by low-speed centrifugation, the phenolic phase was again extracted with an equal volume of water. The two aqueous extracts were combined and residual phenol was removed by extraction with the chloroform. The aqueous phase containing the crude lipoglycans was evaporated to dryness. The crude lipoglycans were subjected to Triton X-114 phase separation (36). The resulting lipoglycans (LAM/LM) were re-suspended in buffer A, 0.2 M NaCl, 0.25% sodium deoxycholate (w/v), 1 mM EDTA and 10 mM Tris, pH 8.0, and loaded onto gel filtration columns (Superdex 75 prep grade column, 50 × 1 cm, Amersham Bioscience) and eluted with buffer A at a flow rate 0.2 ml min^{-1}. The fractions were collected and analyzed by SDS–PAGE followed by silver staining. The LAM and LM fractions pooled were dialyzed extensively against water, lyophilized and stored at −20°C.

Mass spectrometric analysis of lipoglycans LAM and LM

MALDI TOF-MS spectra were acquired on a Voyager DE-STR MALIDI TOF-MS spectrometer (Applied Biosystem) with a pulse laser emitting at 337 nm. The samples were analyzed in the reflectron mode with an accelerating voltage operating in the negative ion mode of 25 kV. As the matrix, 2,5-dihydroxybenzoic acid was used at a concentration of 10 mg ml^{-1}, in a mixture of water. A total of 1.0 μl of lipoglycan, at a concentration of 10 mg ml^{-1}, was mixed with 1.0 μl of the matrix solution. The sample mixture was applied onto the sample plate as a 1.0-μl droplet. The samples were then allowed to crystallize at room temperature.

Preparation of human PBMCs and CD4 T cells

Whole blood was obtained from six healthy donor volunteers between 24 and 50 years old. The protocol was approved by the Institutional Ethics Committee (No. 1972). PBMCs were isolated by Ficol-Paque (Pharmacia-Upjohn, Uppsala, Sweden) gradient centrifugation (37). Naive $CD4^+$ T cells were stained with anti-CD8/CD45RO–FITC and then purified using anti-FITC magnetic beads (Miltenyi Biotec) and AutoMACS cell sorter (Miltenyi Biotec) by negative sorting.

Preparation of highly purified naive CD4 T cells and monocyte derived dendritic cells

Highly purified naive CD4 T cells ($CD4^+$, $CD45RA^+$) were prepared using a human naive CD4 T cell isolation kit (Miltenyi Biotec Inc.) and an AutoMACS sorter. The purity ($CD4^+$, $CD45RA^+$) was >95%. For preparation of monocyte derived dendritic cells, whole PBMCs were allowed to adhere to culture flasks for 1.5–2 h at 37°C and then adherent cells were cultured for 5–7 days in the presence of human IL-4 (500 U ml^{-1}, R&D Systems, Minneapolis, MN, USA) and human granulocyte macrophage colony-stimulating factor (800 U ml^{-1}) (38). $CD11c^+$ cells were purified using a MACS separation column (Miltenyi Biotec) according to the manufacturer's protocol. Purified DCs (7.5 × 10^5 per well) were added to the *in vitro* T cell differentiation culture.

In vitro *T cell differentiation culture*

Naive CD4 T cells or highly purified naive CD4 T cells (7.5 × 10^5 per well) were stimulated with 20 μg ml^{-1} immobilized anti-CD3 mAb (Raritan, Somerset County, NJ, USA) for 2 days in the presence of 50 U ml IL-2 (Shionogi & Co., Ltd, Osaka, Japan), 1 ng ml^{-1} IL-12 (R&D Systems) and 5 μg ml^{-1} anti-IL-4 mAb (BD Bioscience) under T_h1 culture conditions (39). For T_h2 conditions, the cells were stimulated with 20 μg ml^{-1} immobilized anti-CD3 mAb in the presence of

50 U ml^{-1} IL-2, 1 ng ml^{-1} IL-4 (R&D Systems) and 5 μg ml^{-1} anti-IFN-γ mAb (BD Bioscience). For neutral conditions, the cells were stimulated with 20 μg ml^{-1} immobilized anti-CD3 mAb in the presence of 50 U ml^{-1} IL-2. The cells were then transferred to new plates and cultured for another 5 days in the presence of cytokines and antibodies used in the same culture conditions. Since IL-4-producing cells were not induced significantly in a week culture under T_h2 culture conditions, two cycles of the stimulation were used. Where indicated, anti-IL-12 mAb (2 μg ml^{-1}, U-CyTech Biosciences, Utrecht, The Netherlands) was added to the culture. The final concentration of CW, LAM/LM, PIM2 and PIM6 was adjusted to 100 μg ml^{-1}.

Intracellular staining of IL-4 and IFN-γ and flow cytometry analysis

The cultured T cells were re-stimulated with PMA (10 ng ml^{-1}) and ionomycin (1 μM) for 4 h in the presence of 2 μM monensin, which inhibited the secretion of newly produced protein. Next, the cells were fixed with 4% PFA for 10 min at room temperature and were permeabilized with 0.5% Triton X-100 (in 50 mM NaCl, 5 mM EDTA and 0.02% NaN_3, pH7.5) for 10 min on ice. After blocking with 3% BSA in PBS for 15 min, the cells were incubated on ice for 45 min with anti-IFN-γ–FITC, IL-4–PE (BD Bioscience) and CD4–allophycocyanin (BD Bioscience) as described (39). A flow cytometry analysis was performed on FACScalibur® (Becton Dickinson, Franklin Lakes, NJ, USA), and the results were analyzed using the CELLQUEST® software program (Becton Dickinson).

Results

Purification of LAM/LM from BCG Tokyo-172

The experimental procedures to extract LM and LAM from *M. bovis* BCG Tokyo-172 are based on successive detergent and phenolic extractions, thus leading to the recovery of nucleic acid-, protein- and lipid-free materials.

LAM and LM fractions were fully separated and collected by gel filtration chromatography (Fig. 2A). The purity of each component was assessed by SDS–PAGE (Fig. 2B), and the molar ratios of mannose and arabinose in LAM and LM fractions were analyzed by gas chromatography/mass spectrometry (data not shown) and MALDI TOF-MS spectrometry (Fig. 2C and D). The accurate molecular weights of LAM and LM were determined on the basis of the deprotonated ions $[M-H]^-$. As a result, LAMs from *M. bovis* BCG TOKYO-172 was identified to be highly heterogeneous lipoglycans possessing 16–46 mannose residues and 50–60 arabinoses and three acyl groups with the molecular weight ranging from 11 000 to 19 000 Da (Fig. 2C). On the other hand, LM from *M. bovis* BCG Tokyo-172 showed clear $[M-H]^-$ ions in MALDI TOF-MS analysis ranging from m/z 3600 to 8400,

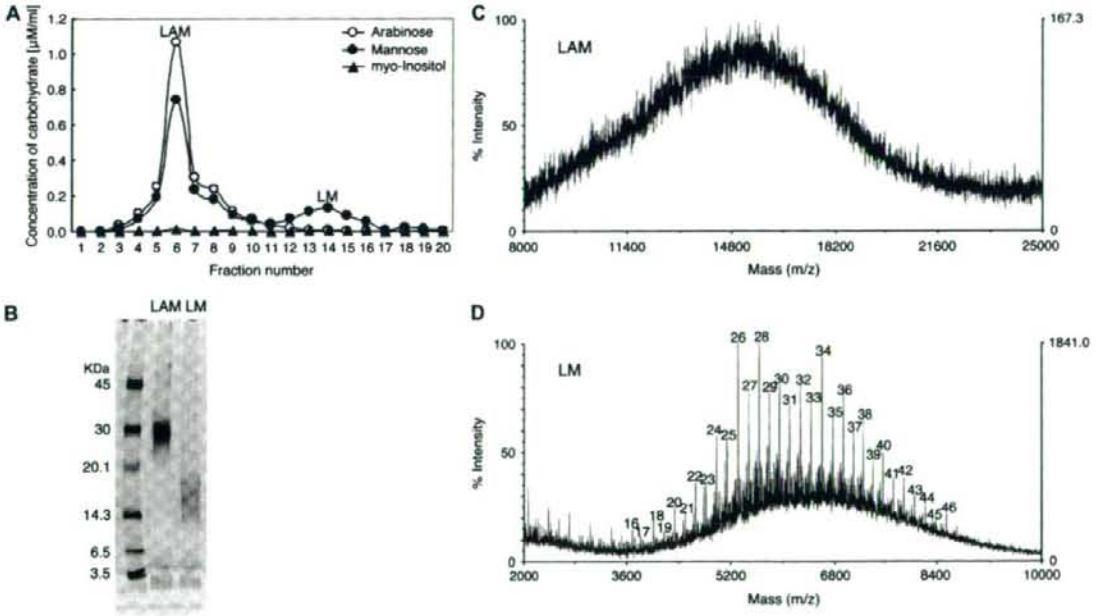

Fig. 2. Purification of BCG Tokyo-172 LAM and LM and MALDI TOF-MS spectra of the purified fractions. (A) Gel filtration profile of the Triton X-114 fraction containing lipoglycans. The fraction was loaded onto a Superdex 75 prep grade column and eluted with deoxycholate buffer. (B) SDS–PAGE analysis of purified fractions from LAM and LM. (C) Negative ion mode MALDI TOF-MS spectra of the fraction LAM. (D) Negative MALDI TOF-MS spectra of the fraction LM that corresponded to triacylated forms, with 2C16 and 1C19 fatty acids. The numbers shown in the figure represent the number of mannose residues in LM.

indicating that they have 16–48 mannoses and three acyl groups, C16:0, C16:0 and C19:0, mainly (Fig. 2D).

Effects of LAM/LM in human T_h1/T_h2 cell differentiation

An *in vitro* T_h1/T_h2 differentiation culture system was used with human peripheral blood naive CD4 T cells to evaluate the effects of BCG CW components on human T_h1/T_h2 differentiation. First, the effect of whole CW fraction and the mixture of LAM/LM were assessed. BCG CW components were homogenously suspended in PBS and then the vehicle was used as negative control. Under T_h1 culture conditions, the generation of T_h1 cells (IFN-γ positive and IL-4 negative) was significantly enhanced in the presence of CW and LAM/LM (37.5 versus 80.7 and 73.6%, respectively) in comparison to the vehicle control (Fig. 3A). Under T_h2 culture conditions, the generation of T_h2 (IL-4 positive and IFN-γ negative) was inhibited significantly in the presence of CW and LAM/LM (25.7 versus 12.5 and 13.9%, respectively), whereas that of T_h1 was enhanced greatly (10.9 versus 37.6 and 38.8%, respectively). Under neutral conditions, they were cultured for 1 week (Fig. 3A) or 2 weeks (Fig. 3B) with anti-CD3 mAb with IL-2, and the generation of IFN-γ-producing T_h1 and that of IL-4-producing T_h2 were marginal, and the levels of these T_h1/T_h2 were not affected in the presence of CW or LAM/LN. These results indicate that CW and LAM/LM enhance T_h1 differentiation and inhibit T_h2 differentiation under both T_h1 and T_h2 culture conditions. Ac4PIM2, Ac3PIM2, Ac4PIM6 and cardiolipin, which are precursors of LAM/LM and cytoplasmic membrane lipids, did not enhance T_h1 differentiation significantly, but showed some induction of T_h2 under T_h2 culture conditions (Fig. 3C), indicating that the precursors of LAM/LM may have different effects from LAM/LM on T_h1/T_h2 differentiation in human PBMC cultures *in vitro* under the given conditions.

Next, to confirm the effects of CW and LAM/LM on T_h1/T_h2 differentiation, the analysis was extended to naive CD4 T cells from 10 healthy volunteers. Similar T_h1/T_h2 cultures were used in the presence of CW and LAM/LM (Fig. 4). As expected, the addition of CW and LAM/LM to the induction culture enhanced T_h1 differentiation under both T_h1 (Fig. 4A and C) and T_h2 culture conditions (Fig. 4B and D, right panels), and the addition of CW suppressed T_h2 differentiation under T_h2 culture conditions (Fig. 4B, left panel) in most of the healthy volunteers tested. The addition of LAM/LM inhibited T_h2 differentiation in some but not all individuals (Fig. 4D, left panel). Thus, these results clearly indicate that CW and LAM/LM enhance T_h1 differentiation while they inhibit T_h2 differentiation. No significant effect was observed under neutral conditions (Supplementary Figure 1, available at *International Immunology* Online). Ac4PIM2, Ac3PIM2, Ac4PIM6 and cardiolipin did not affect the levels of either T_h1 differentiation under both T_h1 and T_h2 culture conditions

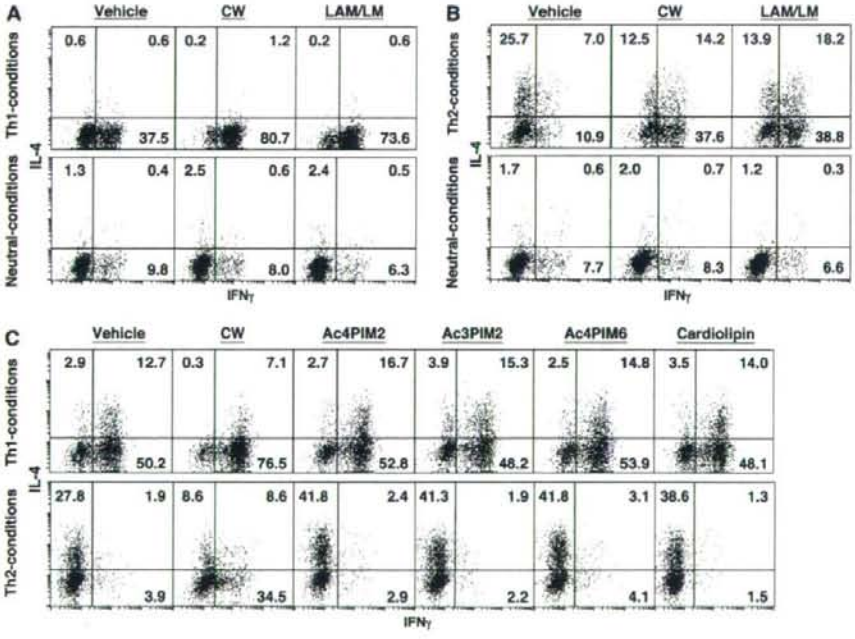

Fig. 3. Effect of BCG CW components on human T_h1/T_h2 differentiation. Naive CD4 T cells from human PBMC were stimulated with anti-CD3 (20 μg ml^{-1}) in the presence of anti-IFN-γ mAb, IL-4 and IL-2 (T_h2 conditions), in the presence of anti-IL-4 mAb, IL-12 and IL-2 (T_h1 conditions) or in the presence of IL-2 (neutral conditions). The cultured cells were subjected to intracellular staining with anti-IL-4 and anti-IFN-γ. A 1-week culture (A) and a 2-week culture (B) were performed. CW and LAM/LM (100 μg ml^{-1}) (A and B) or Ac4PIM2, Ac3PIM2, Ac4PIM6 or cardiolipin (C) (100 μg ml^{-1}) were added to the culture.

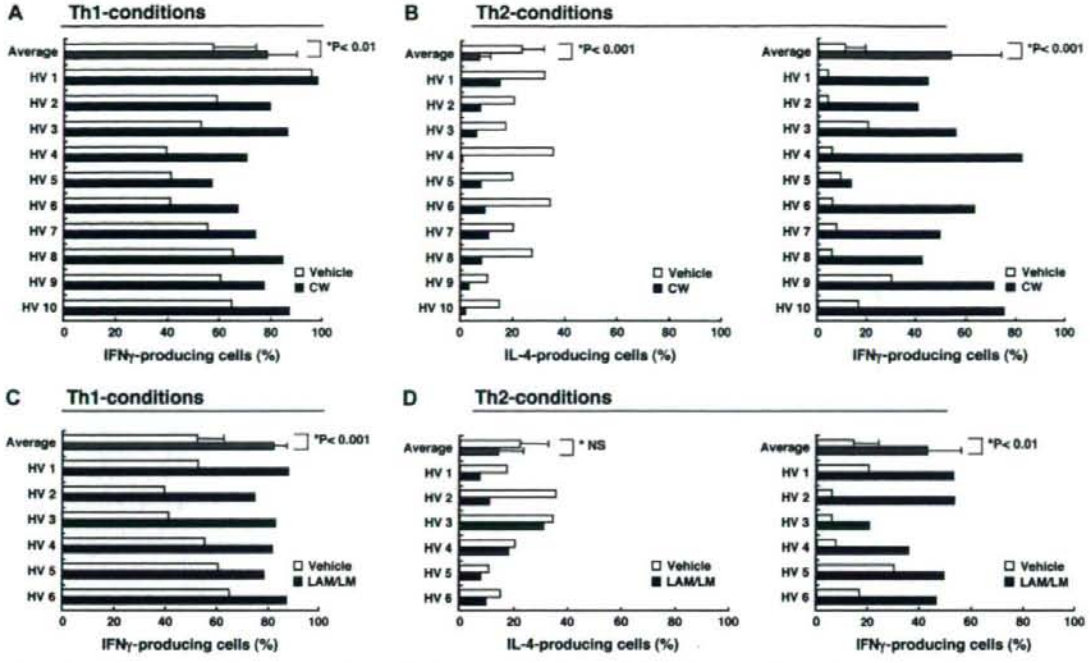

Fig. 4. Effect of BCG CW and LAM/LM on T_h1/T_h2 differentiation using ten human healthy donor PBMCs. T_h1/T_h2 cell differentiation cultures with naive CD4 T cells from 10 human PBMCs were performed as described in Fig. 3. CW (A and B) and LAM/LM (C and D) (100 μg ml^{-1}) were added. The mean values with standard deviations are also shown. Statistical analysis was done using Student's *t*-test.

(Fig. 5A–H). In addition, the effect of these components on the differentiation of T_h2 was seen in some cultures but the effects were marginal (Fig. 5B, D, F and H).

Cellular mechanisms underlying the LAM/LM-mediated modulation of human T_h1/T_h2 differentiation

The CD4 T cells from human PBMC, which were used in the experiments described above, were prepared by removing $CD8^+CD45RO^+$ cells with an AutoMACS cell sorter as described in Methods. These cell preparations contain substantial numbers of forward-$scatter^{high}$/side-$scatter^{high}$ cells and CD4-negative cells (Fig. 6A, Fraction A). To further enrich CD4 T cells, a naive CD4 T cell isolation kit and AutoMACS cell sorter were used (Fig. 6B, Fr. B). Positive cells for CD8, CD14, CD16, CD19, CD36, CD45RO, CD56, CD123, TCRγδ or glycophorin were removed in this separation procedure. Concurrently, CD11c-positive *in vitro* generated DCs from PBMCs were isolated using PE-conjugated anti-CD11c mAb, anti-PE magnetic beads and AutoMACS (Fig. 6C, Fr. C). Using these crude naive CD4 T cells (Fr. A), highly purified naive CD4 T cells (Fr. B) and the mixture of purified naive CD4 T cells (Fr. B) and enriched DCs (Fr. C), T_h1/T_h2 differentiation cultures were set in the presence of LAM/LM (Fig. 7). Under T_h1 culture conditions, the generation of IFN-γ-producing cells was enhanced by LAM/LM in all cultures with Fr. A, Fr. B and the mixture of Fr. B and Fr. C (Fig. 7A, left). Under neutral conditions, the induction of IFN-γ-producing cells was marginal after a 1-week culture with Fr. A and Fr. B, and no significant effect was observed (Fig. 7A, right). However, in the culture of the mixture of purified naive CD4 T cells (Fr. B) and DCs (Fr. C), the generation of IFN-γ-producing cells was enhanced. Under T_h2 culture conditions, the enhancement of the generation of IFN-γ-producing cells and the inhibition of the generation of IL-4-producing cells in the presence of LAM/LM were observed in the cultures with Fr. A but not in the cultures with Fr. B (Fig. 7B, left panels). Interestingly, however, the effects of LAM/LM were restored by the addition of DCs (Fr. C) into purified naive CD4 T cells (Fr. B) (Fig. 7B, left bottom). The addition of anti-IL-12 mAb inhibited the enhancement of the generation of IFN-γ-producing cells (10.3 versus 3.2%) and the suppression of the generation of IL-4-producing cells (24.4 versus 40.3%) in the Fr. A cultures. No effect was observed in the Fr. B cultures (15.8 versus 15.4%). A small but moderate rescue effect was observed in the culture with the mixture of Fr. B and Fr. C (3.1 versus 4.5%). Basically, the same pattern as that seen after the 1-week culture (Fig. 7A, right) was observed after the 2-week culture under neutral conditions (Fig. 7B, right). These results indicate that LAM/LM acts directly to CD4 T cells to enhance the generation of IFN-γ-producing cells under T_h1 culture conditions and that LAM/LM acts indirectly via DCs

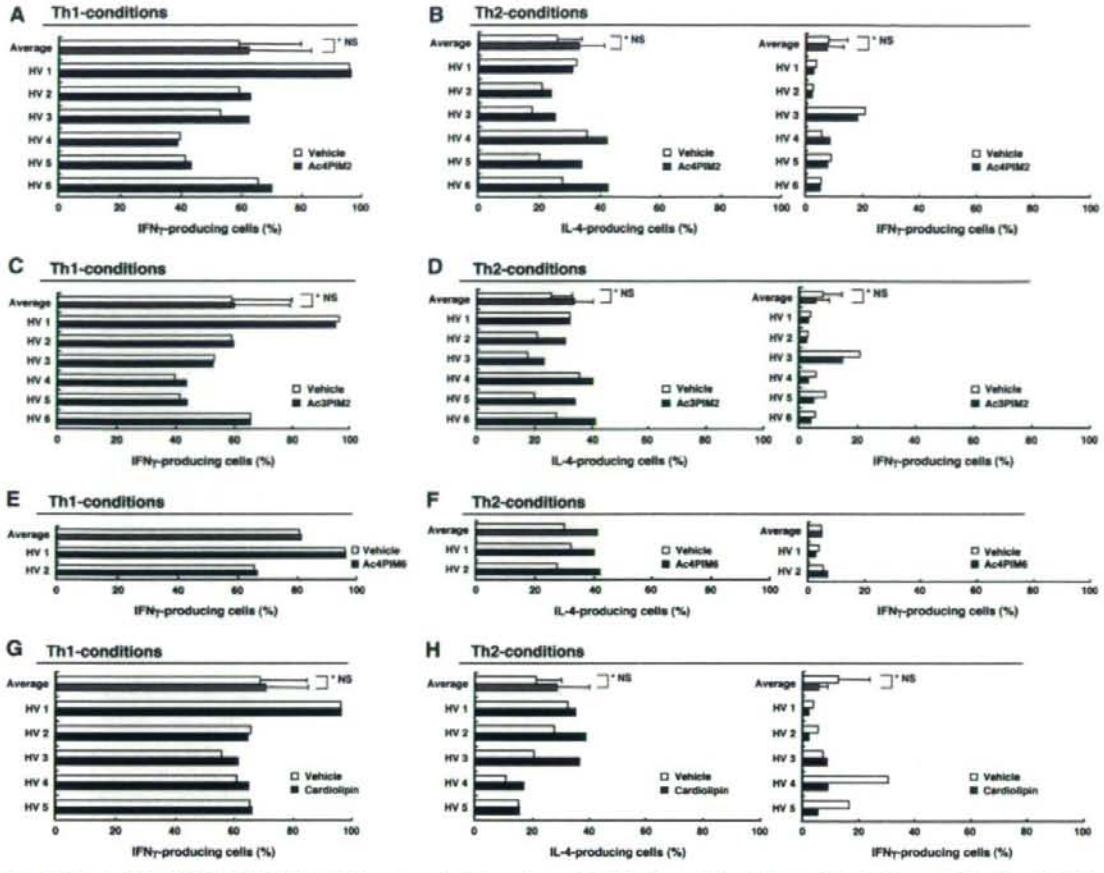

Fig. 5. Effect of Ac4PIM2, Ac3PIM2, Ac4PIM6 and cardiolipin on human T_h1/T_h2 differentiation. Effects of Ac4PIM2 under T_h1 (A) or T_h2 (B) conditions, Ac3PIM2 under T_h1 (C) or T_h2 (D) conditions, Ac4PIM6 under T_h1 (E) or T_h2 (F) conditions and cardiolipin under T_h1 (G) or T_h2 (H) conditions in T_h1/T_h2 differentiation are shown.

to CD4 T cells to enhance the generation of IFN-γ-producing cells and inhibit the generation of IL-4-producing cells under T_h2 culture conditions. IL-12 appears to play an important role in the indirect regulation by LAM/LM.

Effects of purified LAM and LM in human T_h1/T_h2 differentiation cultures

The balance of ManLAM/LM is considered to be important for the protection from mycobacterial infection (34). To further confirm the effects of LAM and LM on the T_h1/T_h2 differentiation, each component was purified from the mixture of LAM/LM and added into the T_h1/T_h2 cultures. Under T_h1 culture conditions, both LAM and LM enhanced the IFN-γ-producing T_h1 cells (58.8 versus 67.3 and 65.5%, respectively), although the levels were slightly lower than those of the cultures with LAM/LM mixture (83.0%; Fig. 8, upper panels). Under T_h2 culture conditions, LAM and LM also induced the generation of IFN-γ-producing T_h1 cells (18.1 versus 35.0 and 29.5%, respectively; Fig. 8, lower panels). No obvious inhibition of the generation of IL-4-producing cells was observed in the presence of LAM or LM. These results indicate that both LAM and LM components possess the ability to enhance T_h1 differentiation. In addition, the balance of LAM/LM may also contribute to the effect on T_h differentiation.

Discussion

The present study using an *in vitro* T_h1/T_h2 differentiation culture system with human peripheral blood naive CD4 T cells demonstrated that LAM/LM from *M. bovis* BCG enhanced T_h1 differentiation by two distinct pathways (Fig. 9). LAM/LM acts directly to naive CD4 T cells to enhance T_h1 cell differentiation under T_h1 culture conditions. LAM/LM also acts indirectly via DCs to induce polarization in T_h differentiation from T_h2 to T_h1 under T_h2 culture conditions.

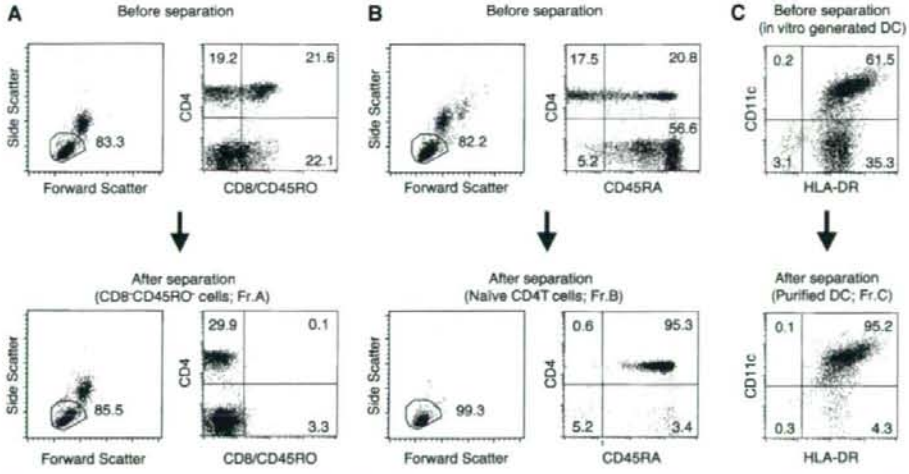

Fig. 6. Enrichment of human naive CD4 T cells and DCs. (A) Isolation of naive CD4 ($CD8^-CD45RO^-$) T cells (Fraction A). Human PBMCs were stained with FITC-conjugated anti-CD8 mAb, FITC-conjugated anti-CD45RO mAb and anti-FITC magnetic beads and then sorted the negative fraction using an AutoMACS® cell sorter. The percentages of cells in each gate are shown. (B) Isolation of purified CD4 T cells (Fr. B). Naive $CD4^+$ T cells were isolated from human PBMCs using human naive $CD4^+$ T cell isolation kit and AutoMACS® cell sorter. The purity of $CD4^+$ cells was 95.3%. (C) Purification of DCs from *in vitro*-generated DCs. *In vitro*-cultured DCs were stained with PE-conjugated anti-CD11c mAb, and the positive fraction of the anti-PE mAb-coupled magnetic beads were purified using an AutoMACS® cell sorter. The purity of the DCs was 95.2%.

It is reported in mouse system that TLRs recognize LMs, and TLR2 play important roles in the induction of type-I inflammatory responses (40–42). The signals via TLR2 induced the expression of CD1 and T cell activation (43). Gilleron *et al.* showed that PIM2 and PIM6, which are the anchor motif of LAM/LM, activate primary macrophages to secrete TNFα through TLR2, irrespective of their acylation pattern (44). These results suggest that PIM2 and PIM6 activate APC via TLR2. In the current study, however, PIM2 and PIM6 did not enhance T_h1 differentiation under T_h1 culture conditions, but enhanced T_h2 differentiation in some individuals under T_h2 culture conditions (Fig. 3C). These results suggest that PIM2 and PIM6 may negatively regulate T_h1 generation through the enhanced differentiation of T_h2 under T_h2 conditions. The discrepancies in the response of APC against PIM2 and PIM6 may be due to the difference in the physicochemical properties of micelle sizes or the solvent used between the PIM products of Gilleron *et al.* (44) and ours. The former PIMs are less polar than that of LAM/LM and produce larger micelle particles in the endocytotic process. In any event, it is likely that LAM/LM stimulates DCs via TLR2 and modifies the balance of T_h1/T_h2 differentiation.

To examine the cellular mechanisms underlying the effect of LAM/LM on the T_h1/T_h2 differentiation, the results with a crude naive CD4 T cell fraction and a highly purified naive CD4 T cell fraction after eliminating APCs were compared. Interestingly, the enhanced generation of T_h1 by LAM/LM under T_h1 culture conditions can be seen markedly in the absence of APCs, but the inhibition of T_h2 generation under T_h2 culture conditions is totally dependent on APCs (Fig. 7). Human CD4 T cells express various types of TLRs including TLR2, 5 and 7/8 (45). In another report, human naive CD4 T cells were found to express undetectable levels of TLR2 but the expression was significantly increased after anti-CD3 stimulation (46). The expression of TLRs was examined in our purified CD4 T cells and it was revealed that the purified CD4 T cells express substantial mRNA levels of TLR1, 2, 5, 7, 9 and 10 (Ito, T. and Nakayame, T., unpublished observation). Thus, it is likely that LAM/LM binds directly to one of these TLRs and induces polarization toward T_h1 differentiation. Recently, in a mouse system, stimulation through TLR2 on T_h1 cells was observed to induce IFN-γ production and proliferation, and this effect is augmented by IL-2 or IL-12 (47). Thus, it is likely that LAM/LM acts on early activated CD4 T cells and also on developing T_h1 in the culture and resulted in the polarized T_h1 differentiation.

In the cultures under neutral conditions, the cytokine autoregulatory loops may proceed, and the effects observed under neutral conditions may be more reflective of the *in vivo* effects of LAM/LM. Unfortunately, in human CD4 T cell cultures, the differentiation of naive T cells into T_h1/T_h2 cells was not efficiently observed under neutral conditions, and no obvious effect of LAM/LM was detected (Figs 3 and 7). However, we observed increases in the generation of IFN-γ-producing cells when we added DCs to the purified CD4 T cell cultures (Fig. 7). Based on these results, we concluded that even under neutral conditions, LAM/LM has an enhancing effect on the generation of IFN-γ-producing T_h1. We will investigate the effect of LAM/LM in the presence of various kinds of DCs under neutral conditions in the near future.

It is possible that NKT cells play a role in the observed LAM/LM-mediated induction of T_h1 differentiation (48, 49). However, during the process of the magnetic separation of $CD8^-CD45RO^-$ cells (naive CD4 T cells, Fr. A in Fig. 6A), all

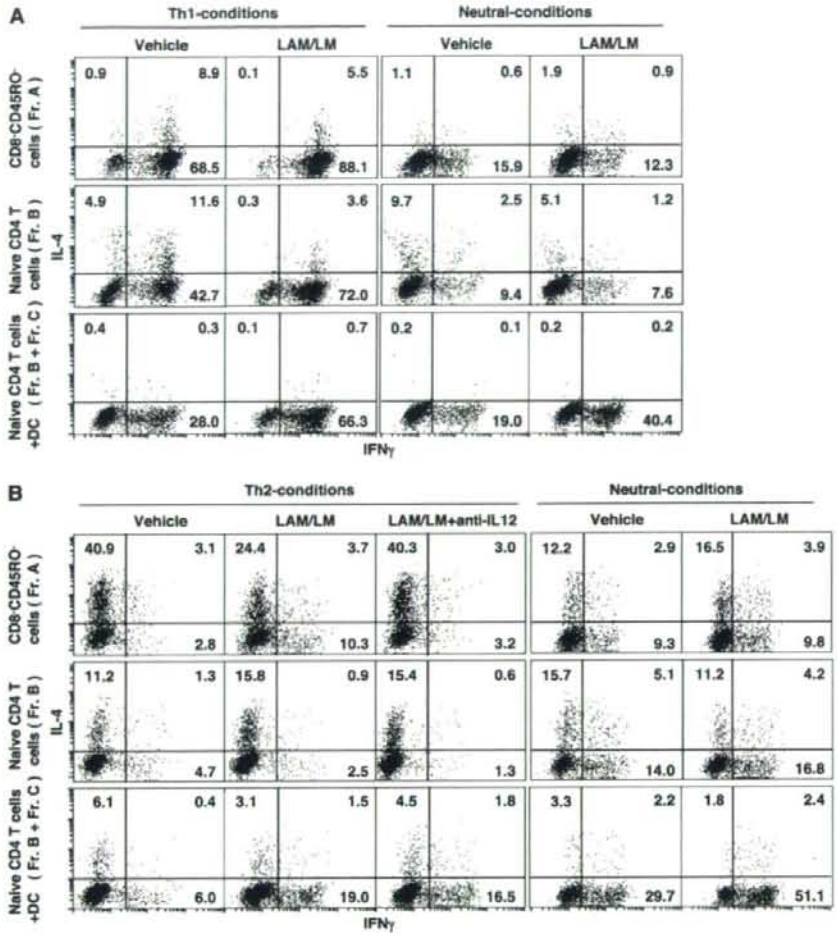

Fig. 7. Roles of DCs in the effect of LAM/LM on T_h1/T_h2 differentiation. Naive CD4 T cells ($CD8^-CD45RO^-$ cells) (Fr. A), purified CD4 T cells (Fr. B) and purified CD4 T cells (Fr. B) and DCs (Fr. C) were stimulated with anti-CD3 under T_h1 (panel A, cultured for a week), T_h2 (panel B, cultured for 2 weeks) or neutral culture conditions (panels A and B, cultured for 1 or 2 weeks, respectively). Anti-IL-12 mAb was added at the beginning of T_h2 cultures. Intracellular staining profiles of IFN-γ/IL-4 are shown with percentages of cells in each area. Three experiments were performed with similar results.

Vα24 NKT cells appeared to be eliminated and undetectable in our preparing naive CD4 T cells (Ito, T. and Nakayama, T., unpublished observation). Therefore, it is unlikely that Vα24 NKT cells are involved in the LAM/LM-mediated induction of T_h1 differentiation.

There are three types of capping motifs in LAM molecules. One is named ManLAM having a mannosyl cap, and this is isolated from *M. tuberculosis* and *M. bovis* including BCG subspecies and *Mycobacterium kansasii*. Another is PILAM, which has a phosphoinositol cap, and is isolated from *M. smegmatis*. The third one is AraLAM, which has no capping motif, and is isolated from *Mycobacterium chelonae* (44). It is reported that LAM and PILAM but not ManLAM or AraLAM activate macrophages and DCs to secrete IL-12 (26, 50, 51). On the other hand, LM but not PIM induces apoptosis or activates these cells to secrete IL-12 (25, 52). These results may indicate that ManLAM possesses the ability to inhibit LM-induced apoptosis and IL-12 secretion. In the present study, both LAM and LM components showed the enhancing activity of T_h1 differentiation (Fig. 8). However, we did not detect any inhibiting effects on the generation of IL-4-producing T_h2 (Fig. 8). We think that the inhibition of the generation of IL-4-secreting cells is a secondary effect by the enhancement of the generation of IFN-γ-producing cells because the inhibition was neutralized by the addition of anti-IL-12 mAb (Fig. 7). Since the effects of LAM and LM on the generation of IFN-γ-producing cells were milder than LAM/LM, we may not be able to detect the inhibition of the

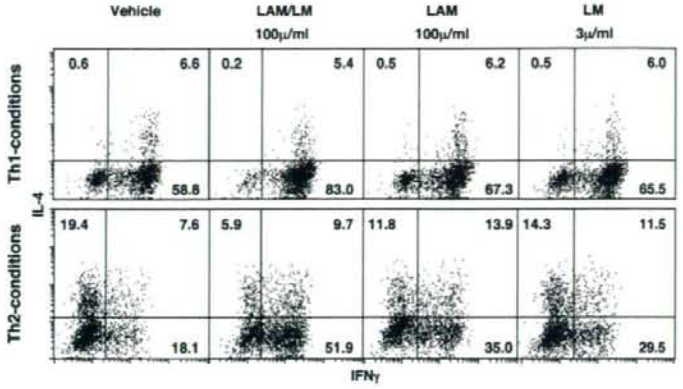

Fig. 8. Effects of purified LAM or LM components on human PBMC T_h1/T_h2 differentiation. Naive CD4 T cells from human PBMC were cultured with LAM/LM (100 μg ml^{-1}), LAM (30 and 100 μg ml^{-1}) or LM (3 and 30 μg ml^{-1}) under T_h1/T_h2 cultured conditions. The intracellular staining profiles of IFN-γ/IL-4 are shown with percentages of cells in each area. Three experiments were performed with similar results.

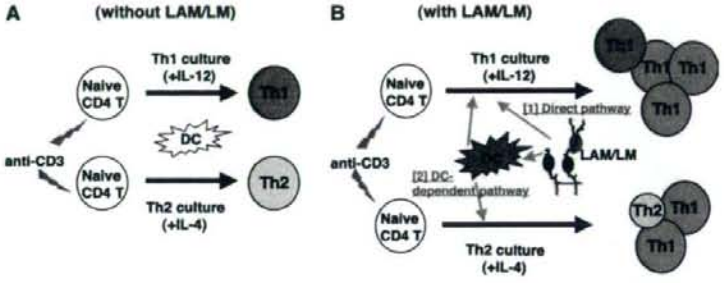

Fig. 9. Two distinct regulatory pathways for T_h1 generation induced by LAM/LM in human T_h1/T_h2 cultures. In the presence of LAM/LM, the generation of T_h1 cells was enhanced both under T_h1 culture conditions and T_h2 culture conditions (panel B). Under T_h1 conditions, LAM/LM directly act on CD4 T cells (direct pathway). LAM/LM act on DCs (DC-dependent pathway) and then induce the enhancement of T_h1 differentiation under both T_h1 and T_h2 conditions.

production of IL-4-secreting cells by LAM or LM (Fig. 8). LM appears to induce T_h1 differentiation more prominently in lower doses than LAM (Ito, T., and Nakayama, T., unpublished observation). In addition, high doses of LM did not show the enhancing effect in T_h1 differentiation (Ito, T., and Nakayama, T., unpublished observation). These results may suggest that the balance of LAM/LM is critically important for the induction of T_h1 responses. Further investigations on the effect of the balance of LAM/LM in the human immune system may contribute to the development of new immunotherapeutic approaches for allergic diseases, cancer and infections diseases.

Supplementary data

Supplementary Figure 1 available at *International Immunology* Online.

Funding

Ministry of Education, Culture, Sports, Science and Technology (Japan) [Grants-in-Aid: for Scientific Research on Priority Areas #17016010; Scientific Research (B) #17390139, Scientific Research (C) #18590466, #19590491 and #19591609, Exploratory Research #19659121 and Young Scientists (Start-up) #18890046; Special Coordination Funds for Promoting Science and Technology and Cancer Translational Research Project]; Ministry of Health, Labor and Welfare (Japan); The Japan Health Science Foundation; Kanae Foundation; Uehara Memorial Foundation; Mochida Foundation; Yasuda Medical Foundation; Astellas Foundation; Sagawa Foundation.

Acknowledgements

We thank Kaoru Sugaya, Hikari Asou and Satoko Norikane for their excellent technical assistance.

Abbreviations

APC	antigen presenting cell
BCG	Bacille Calmett–Guerin
CW	cell wall
DC	dendritic cell
LAM	lipoarabinomannan

LM	lipomannan
ManLAM	LAM with mannose caps
PI	phosphatidylinositol
PIM	phosphatidylinositol mannosides
PIM2	phosphatidylinositol dimannoside
PIM6	phosphatidylinositol hexamannoside
TLR2	Toll-like receptor 2
TNFα	tumor necrosis factor α

References

1 Besra, G. S., Morehouse, C. B., Rittner, C. M., Waechter, C. J. and Brennan, P. J. 1997. Biosynthesis of mycobacterial lipoarabinomannan. *J. Biol. Chem.* 272:18460.

2 Nigou, J., Gilleron, M. and Puzo, G. 1999. Lipoarabinomannans: characterization of the multiacylated forms of the phosphatidyl-*myo*-inositol anchor by NMR spectroscopy. *Biochem. J.* 337:453.

3 Sibley, L. D., Hunter, S. W., Brennan, P. J. and Krahenbuhl, J. L. 1988. Mycobacterial lipoarabinomannan inhibits gamma interferon-mediated activation of macrophages. *Infect. Immun.* 56:1232.

4 Sibley, L. D., Adams, L. B. and Krahenbuhl, J. L. 1990. Inhibition of interferon-gamma-mediated activation in mouse macrophages treated with lipoarabinomannan. *Clin. Exp. Immunol.* 80:141.

5 Moreno, C., Mehlert, A. and Lamb, J. 1988. The inhibitory effects of mycobacterial lipoarabinomannan and polysaccharides upon polyclonal and monoclonal human T cell proliferation. *Clin. Exp. Immunol.* 74:206.

6 Chan, J., Fan, X. D., Hunter, S. W., Brennan, P. J. and Bloom, B. R. 1991. Lipoarabinomannan, a possible virulence factor involved in persistence of *Mycobacterium tuberculosis* within macrophages. *Infect. Immun.* 59:1755.

7 Schlesinger, L. S., Hull, S. R. and Kaufman, T. M. 1994. Binding of the terminal mannosyl units of lipoarabinomannan from a virulent strain of *Mycobacterium tuberculosis* to human macrophages. *J. Immunol.* 152:4070.

8 Apostolou, I., Takahama, Y., Belmant, C. *et al.* 1999. Murine natural killer T(NKT) cells [correction of natural killer cells] contribute to the granulomatous reaction caused by mycobacterial cell walls. *Proc. Natl Acad. Sci. USA* 96:5141.

9 Gilleron, M., Ronet, C., Mempel, M., Monsarrat, B., Gachelin, G. and Puzo, G. 2001. Acylation state of the phosphatidylinositol mannosides from *Mycobacterium bovis* bacillus Calmette Guerin and ability to induce granuloma and recruit natural killer T cells. *J. Biol. Chem.* 276:34896.

10 Khoo, K. H., Dell, A., Morris, H. R., Brennan, P. J. and Chatterjee, D. 1995. Structural definition of acylated phosphatidylinositol mannosides from *Mycobacterium tuberculosis*: definition of a common anchor for lipomannan and lipoarabinomannan. *Glycobiology.* 5:117.

11 Schaeffer, M. L., Khoo, K. H., Besra, G. S. *et al.* 1999. The *pimB* gene of *Mycobacterium tuberculosis* encodes a mannosyltransferase involved in lipoarabinomannan biosynthesis. *J. Biol. Chem.* 274:31625.

12 Kremer, L., Gurcha, S. S., Bifani, P. *et al.* 2002. Characterization of a putative α-mannosyltransferase involved in phosphatidylinositol trimannoside biosynthesis in *Mycobacterium tuberculosis*. *Biochem. J.* 363:437.

13 Hunter, S. W. and Brennan, P. J. 1990. Evidence for the presence of a phosphatidylinositol anchor on the lipoarabinomannan and lipomannan of *Mycobacterium tuberculosis*. *J. Biol. Chem.* 265:9272.

14 Banchereau, J. and Steinman, R. M. 1998. Dendritic cells and the control of immunity. *Nature* 392:245.

15 Cella, M., Sallusto, F. and Lanzavecchia, A. 1997. Origin, maturation and antigen presenting function of dendritic cells. *Curr. Opin. Immunol.* 9:10.

16 Reis e Sousa, C., Sher, A. and Kaye, P. 1999. The role of dendritic cells in the induction and regulation of immunity to microbial infection. *Curr. Opin. Immunol.* 11:392.

17 Demangel, C., Bean, A. G., Martin, E., Feng, C. G., Kamath, A. T. and Britton, W. J. 1999. Protection against aerosol *Mycobacterium tuberculosis* infection using *Mycobacterium bovis* Bacillus Calmette Guerin-infected dendritic cells. *Eur. J. Immunol.* 29:1972.

18 Thurnher, M., Ramoner, R., Gastl, G. *et al.* 1997. Bacillus Calmette-Guerin mycobacteria stimulate human blood dendritic cells. *Int. J. Cancer.* 70:128.

19 Tascon, R. E., Soares, C. S., Ragno, S., Stavropoulos, E., Hirst, E. M. and Colston, M. J. 2000. *Mycobacterium tuberculosis*-activated dendritic cells induce protective immunity in mice. *Immunology.* 99:473.

20 Cooper, A. M., Dalton, D. K., Stewart, T. A., Griffin, J. P., Russell, D. G. and Orme, I. M. 1993. Disseminated tuberculosis in interferon γ gene-disrupted mice. *J. Exp. Med.* 178:2243.

21 Flynn, J. L., Chan, J., Triebold, K. J., Dalton, D. K., Stewart, T. A. and Bloom, B. R. 1993. An essential role for interferon γ in resistance to *Mycobacterium tuberculosis* infection. *J. Exp. Med.* 178:2249.

22 Dalton, D. K., Haynes, L., Chu, C. Q., Swain, S. L. and Wittmer, S. 2000. Interferon γ eliminates responding CD4 T cells during mycobacterial infection by inducing apoptosis of activated CD4 T cells. *J. Exp. Med.* 192:117.

23 Li, X., McKinstry, K. K., Swain, S. L. and Dalton, D. K. 2007. IFN-γ acts directly on activated $CD4^+$ T cells during mycobacterial infection to promote apoptosis by inducing components of the intracellular apoptosis machinery and by inducing extracellular proapoptotic signals. *J. Immunol.* 179:939.

24 Ottenhoff, T. H., Kumararatne, D. and Casanova, J. L. 1998. Novel human immunodeficiencies reveal the essential role of type-I cytokines in immunity to intracellular bacteria. *Immunol. Today.* 19:491.

25 Nigou, J., Zelle-Rieser, C., Gilleron, M., Thurnher, M. and Puzo, G. 2001. Mannosylated lipoarabinomannans inhibit IL-12 production by human dendritic cells: evidence for a negative signal delivered through the mannose receptor. *J. Immunol.* 166:7477.

26 Geijtenbeek, T. B., Van Vliet, S. J., Koppel, E. A. *et al.* 2003. Mycobacteria target DC-SIGN to suppress dendritic cell function. *J. Exp. Med.* 197:7.

27 Tailleux, L., Maeda, N., Nigou, J., Gicquel, B. and Neyrolles, O. 2003. How is the phagocyte lectin keyboard played? Master class lesson by *Mycobacterium tuberculosis*. *Trends Microbiol.* 11:259.

28 Gilleron, M., Himoudi, N., Adam, O. *et al.* 1997. *Mycobacterium smegmatis* phosphoinositols-glyceroarabinomannans. Structure and localization of alkali-labile and alkali-stable phosphoinositides. *J. Biol. Chem.* 272:117.

29 Adams, L. B., Fukutomi, Y. and Krahenbuhl, J. L. 1993. Regulation of murine macrophage effector functions by lipoarabinomannan from mycobacterial strains with different degrees of virulence. *Infect. Immun.* 61:4173.

30 Means, T. K., Lien, E., Yoshimura, A., Wang, S., Golenbock, D. T. and Fenton, M. J. 1999. The CD14 ligands lipoarabinomannan and lipopolysaccharide differ in their requirement for Toll-like receptors. *J. Immunol.* 163:6748.

31 Vignal, C., Guerardel, Y., Kremer, L. *et al.* 2003. Lipomannans, but not lipoarabinomannans, purified from *Mycobacterium chelonae* and *Mycobacterium kansasii* induce TNF-α and IL-8 secretion by a CD14-toll-like receptor 2-dependent mechanism. *J. Immunol.* 171:2014.

32 Quesniaux, V. J., Nicolle, D. M., Torres, D. *et al.* 2004. Toll-like receptor 2 (TLR2)-dependent-positive and TLR2-independent-negative regulation of proinflammatory cytokines by mycobacterial lipomannans. *J. Immunol.* 172:4425.

33 Dao, D. N., Kremer, L., Guerardel, Y. *et al.* 2004. *Mycobacterium tuberculosis* lipomannan induces apoptosis and interleukin-12 production in macrophages. *Infect. Immun.* 72:2067.

34 Briken, V., Porcelli, S. A., Besra, G. S. and Kremer, L. 2004. Mycobacterial lipoarabinomannan and related lipoglycans: from biogenesis to modulation of the immune response. *Mol. Microbiol.* 53:391.

35 Fujita, Y., Doi, T., Sato, K. and Yano, I. 2005. Diverse humoral immune responses and changes in IgG antibody levels against mycobacterial lipid antigens in active tuberculosis. *Microbiology.* 151:2065.

36 Nigou, J., Gilleron, M., Cahuzac, B. *et al.* 1997. The phosphatidyl-*myo*-inositol anchor of the lipoarabinomannans from *Mycobacterium*

bovis bacillus Calmette Guerin. Heterogeneity, structure, and role in the regulation of cytokine secretion. *J. Biol. Chem.* 272:23094.
37 Motohashi, S., Kobayashi, S., Ito, T. *et al.* 2002. Preserved IFN-α production of circulating Vα24 NKT cells in primary lung cancer patients. *Int. J. Cancer.* 102:159.
38 Ishikawa, E., Motohashi, S., Ishikawa, A. *et al.* 2005. Dendritic cell maturation by CD11c− T cells and Vα24$^+$ natural killer T-cell activation by α-galactosylceramide. *Int. J. Cancer.* 117:265.
39 Kaneko, T., Hosokawa, H., Yamashita, M. *et al.* 2007. Chromatin remodeling at the Th2 cytokine gene loci in human type 2 helper T cells. *Mol. Immunol.* 44:2249.
40 Fricke, I., Mitchell, D., Mittelstadt, J. *et al.* 2006. Mycobacteria induce IFN-γ production in human dendritic cells via triggering of TLR2. *J. Immunol.* 176:5173.
41 Gilleron, M., Nigou, J., Nicolle, D., Quesniaux, V. and Puzo, G. 2006. The acylation state of mycobacterial lipomannans modulates innate immunity response through toll-like receptor 2. *Chem. Biol.* 13:39.
42 Dabbagh, K. and Lewis, D. B. 2003. Toll-like receptors and T-helper-1/T-helper-2 responses. *Curr. Opin. Infect. Dis.* 16:199.
43 Roura-Mir, C., Wang, L., Cheng, T. Y. *et al.* 2005. *Mycobacterium tuberculosis* regulates CD1 antigen presentation pathways through TLR-2. *J. Immunol.* 175:1758.
44 Nigou, J., Gilleron, M. and Puzo, G. 2003. Lipoarabinomannans: from structure to biosynthesis. *Biochimie.* 85:153.
45 Kabelitz, D. 2007. Expression and function of Toll-like receptors in T lymphocytes. *Curr. Opin. Immunol.* 19:39.
46 Xu, D., Kornai-Korna, M. and Liew, F. Y. 2005. Expression and function of Toll-like receptor on T cells. *Cell. Immunol.* 233:85.
47 Imanishi, T., Hara, H., Suzuki, S., Suzuki, N., Akira, S. and Saito, T. 2007. Cutting edge: tLR2 directly triggers Th1 effector functions. *J. Immunol.* 178:6715.
48 Emoto, M., Emoto, Y., Buchwalow, I. B. and Kaufmann, S. H. 1999. Induction of IFN-γ-producing CD4$^+$ natural killer T cells by *Mycobacterium bovis* bacillus Calmette Guerin. *Eur. J. Immunol.* 29:650.
49 Dieli, F., Taniguchi, M., Kronenberg, M. *et al.* 2003. An anti-inflammatory role for Vα14 NK T cells in *Mycobacterium bovis* bacillus Calmette-Guerin-infected mice. *J. Immunol.* 171:1961.
50 Rojas, M., Garcia, L. F., Nigou, J., Puzo, G. and Olivier, M. 2000. Mannosylated lipoarabinomannan antagonizes *Mycobacterium tuberculosis*-induced macrophage apoptosis by altering Ca^{+2}-dependent cell signaling. *J. Infect. Dis.* 182:240.
51 Yoshida, A. and Koide, Y. 1997. Arabinofuranosyl-terminated and mannosylated lipoarabinomannans from *Mycobacterium tuberculosis* induce different levels of interleukin-12 expression in murine macrophages. *Infect. Immun.* 65:1953.
52 Nigou, J., Gilleron, M., Rojas, M., Garcia, L. F., Thurnher, M. and Puzo, G. 2002. Mycobacterial lipoarabinomannans: modulators of dendritic cell function and the apoptotic response. *Microbes Infect.* 4:945.

Published November 17, 2008

JEM

BRIEF DEFINITIVE REPORT

A novel subset of mouse NKT cells bearing the IL-17 receptor B responds to IL-25 and contributes to airway hyperreactivity

Asuka Terashima,[1] Hiroshi Watarai,[1] Sayo Inoue,[1] Etsuko Sekine,[1] Ryusuke Nakagawa,[1] Koji Hase,[2] Chiaki Iwamura,[3] Hiroshi Nakajima,[4] Toshinori Nakayama,[3] and Masaru Taniguchi[1]

[1]Laboratory for Immune Regulation and [2]Laboratory for Epithelial Immunobiology, RIKEN Research Center for Allergy and Immunology, Tsurumi-ku, Yokohama, Kanagawa, 230-0045, Japan
[3]Department of Immunology and [4]Department of Molecular Genetics, Graduate School of Medicine, Chiba University, Chuo-ku, Chiba, 260-8670, Japan

Airway hypersensitive reaction (AHR) is an animal model for asthma, which is caused or enhanced by environmental factors such as allergen exposure. However, the precise mechanisms that drive AHR remain unclear. We identified a novel subset of natural killer T (NKT) cells that expresses the interleukin 17 receptor B (IL-17RB) for IL-25 (also known as IL-17E) and is essential for the induction of AHR. IL-17RB is preferentially expressed on a fraction of CD4$^+$ NKT cells but not on other splenic leukocyte populations tested. IL-17RB$^+$ CD4$^+$ NKT cells produce predominantly IL-13 and Th2 chemokines upon stimulation with IL-25 in vitro. IL-17RB$^+$ NKT cells were detected in the lung, and depletion of IL-17RB$^+$ NKT cells by IL-17RB–specific monoclonal antibodies or NKT cell–deficient Jα18$^{-/-}$ mice failed to develop IL-25–dependent AHR. Cell transfer of IL-17RB$^+$ but not IL-17RB$^-$ NKT cells into Jα18$^{-/-}$ mice also successfully reconstituted AHR induction. These results strongly suggest that IL-17RB$^+$ CD4$^+$ NKT cells play a crucial role in the pathogenesis of asthma.

CORRESPONDENCE
Hiroshi Watarai:
hwatarai@rcai.riken.jp

Airway hypersensitive reaction (AHR) (1) is known to be associated with Th2 cytokines—including IL-4, IL-5, and IL-13—regulating effector functions (2). Indeed, overexpression of these Th2 cytokines results in the development of AHR (3). However, efforts to ameliorate experimental asthma with antibodies against Th2 cytokines have generally proven unsuccessful. Among these, only IL-13 seems to be a key cytokine responsible for goblet cell hyperplasia, airway remodeling, and AHR (4), because inhibition of IL-13 activity, but not that of other Th2 cytokines, by a blocking antibody suppresses both AHR and airway inflammation.

IL-25 (also known as IL-17E), a member of the structurally related IL-17 cytokine family (5–7), has recently been reported to be produced by activated Th2 cells (5) and mast cells (8), resulting in enhancement of AHR (9, 10). Administration of a blocking antibody against IL-25 (11) or IL-25–deficient mice (12) eliminates Th2 responses. Conversely, systemic expression of either human (7) or mouse (11) IL-25, or administration of recombinant IL-25 (5), induces Th2-type immune responses, including increased serum IgE levels, blood eosinophilia, and pathological changes in the lung and other tissues. These findings clearly demonstrate a pivotal role of IL-25 as a mediator of Th2 responses, suggesting that IL-25 lies upstream of the classical Th2 cytokine responses (5, 11).

NKT cells characterized by the expression of an invariant antigen receptor encoded by *Vα14Jα18* in mice or *Vα24Jα18* in humans are also involved in the development of asthma, because NKT cell–deficient Jα18$^{-/-}$ mice fail to develop antigen-induced AHR (13). Th2 cells are not always essential for NKT cell–mediated AHR development, because activation of NKT cells induces AHR in the absence of CD4$^+$ T

A. Terashima and H. Watarai contributed equally to this paper.
The online version of this article contains supplemental material.

The Rockefeller University Press $30.00
J. Exp. Med. Vol. 205 No. 12 2727-2733
www.jem.org/cgi/doi/10.1084/jem.20080698

Supplemental Material can be found at:
http://jem.rupress.org/cgi/content/full/jem.20080698/DC1

The Journal of Experimental Medicine

Published November 17, 2008

cells in *MHC class II*–deficient mice (14). These findings suggest that NKT cells are directly involved in the development of AHR independent of Th2 responses in some conditions. In this report, we investigated the role of IL-25 in NKT cell–dependent AHR induction in mouse models and found that IL-17RB, a receptor for IL-25, was selectively expressed on a fraction of mouse NKT cells, which preferentially produced IL-13 and induced the development of AHR upon stimulation with IL-25.

RESULTS AND DISCUSSION

We first investigated the role of IL-25 in the development of AHR in relation to NKT cells because of previous findings that IL-25 induces Th2-biased responses (5–7). The receptor for IL-25, termed IL-17RB or EVI27/IL-17BR, was originally found to bind IL-17B (15). Interestingly, however, the receptor binds IL-25 with higher affinity than IL-17B. Therefore, this receptor is now termed IL-17RB/IL-25R (15). To identify mouse IL-17RB$^+$ cells, we generated specific mAbs (Fig. S1, available at http://www.jem.org/cgi/content/full/jem.20080698/DC1) by immunization with a recombinant IL-17RB–Ig fusion protein (Fig. S2). We first investigated IL-17RB$^+$ cells in the spleen by mouse IL-17RB mAb to confirm the previous findings that IL-17RB expression is detected on a fraction of non–B/non–T (NBNT), c-kit$^+$, FcεRI$^-$ cells in the mesenteric lymph node (Fig. S3), which has identified as IL-4–, IL-5–, IL-13–producing cells in response to IL-25 (12). NKT cells were distinct from the NBNT c-kit$^+$ cells based on the expression of c-kit$^-$, FcεRI$^-$, Vα14-Jα18$^+$ transcripts detected by RT-PCR (Fig. S4). Moreover, IL-17RB was preferentially expressed on a fraction of α-galactosylceramide (α-GalCer)/CD1d dimer$^+$ NKT cells but not on other cell types, including NBNT c-kit$^+$ cells, CD4$^+$ T cells, CD8$^+$ T cells, γδ$^+$ T cells, CD19$^+$ B cells, CD11c$^+$ DCs, DX5$^+$ NK cells, or noninvariant NKT cells in the spleen (Fig. 1 A).

The preferential expression of IL-17RB in a fraction of NKT cells raises a question about the phenotypic and functional

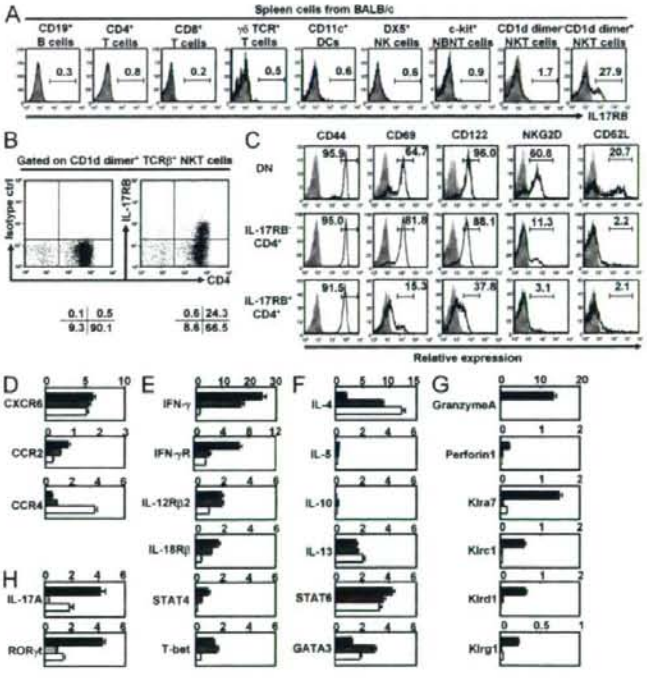

Figure 1. Phenotypic and gene expression profiles of splenic IL-17RB$^+$ NKT cells. (A) Identification of IL-17RB$^+$ cells from BALB/c mice. The indicated populations were gated and analyzed by FACS using F(ab')$_2$ fragments of the anti–IL-17RB mAb B5F6. Shaded profiles in the histograms indicate the background staining with rat F(ab')$_2$ IgG2a. (B) FACS profile of CD1d dimer$^+$ NKT cells stained with anti-CD4 and anti–IL-17RB. (C) Surface phenotype of DN, IL-17RB$^-$ CD4$^+$, and IL-17RB$^+$ CD4$^+$ NKT cells indicated in B. Shaded profiles in the histograms indicate the background staining with isotype-matched control antibody. Percentages are shown. (D–H) Quantitative analyses of genes for chemokine receptors (D), Th1-related molecules (E), Th2-related molecules (F), cytotoxic molecules (G), and Th17-related molecules (H) in isolated DN (black bars), IL-17RB$^-$ CD4$^+$ (gray bars), and IL-17RB$^+$ CD4$^+$ (white bars) NKT cells. Expression of each mRNA was determined by quantitative real-time PCR using the primer sets shown in Table S1 (available at http://www.jem.org/cgi/content/full/jem.20080698/DC1) and is depicted as the number of transcripts per one copy of the housekeeping gene HPRT. One representative out of three experiments is shown (means ± SEM).

Published November 17, 2008

characteristics of these cells. Based on our current understanding, NKT cells are divided into two populations based on CD4/CD8 expression: a $CD4^+$ and a $CD4^-CD8^-$ double-negative (DN) population (16). Using an IL-17RB mAb, we found that one third of the $CD4^+$ but none of the DN NKT cells expressed IL-17RB, indicating the existence of three subpopulations: DN, IL-17RB$^-$ $CD4^+$, and IL-17RB$^+$ $CD4^+$ NKT cells (Fig. 1 B). Moreover, the majority of IL-17RB$^+$ NKT cells were dimly positive for CD69 and CD122 compared with brightly positive DN NKT and IL-17RB$^-$ $CD4^+$ NKT cells (Fig. 1 C). The expression level of CD62L by IL-17RB$^+$ NKT cells was low, comparable to that on IL-17RB$^-$ $CD4^+$ NKT cells and similar to that of conventional memory T cells, whereas it was quite high on DN NKT cells. In addition, IL-17RB$^+$ NKT cells (3%), like IL-17RB$^-$ $CD4^+$ NKT cells (11%), barely expressed an NK receptor, NKG2D, which was highly expressed on the majority (>60%) of DN NKT cells, suggesting their cytotoxic nature (17).

To investigate cytokine and chemokine gene expression profiles on IL-17RB$^+$ NKT cells, we performed quantitative real-time PCR using primer sets as shown in Table S1 (available at http://www.jem.org/cgi/content/full/jem.20080698/DC1). The expression of the Th2 chemokine receptor *CCR4* was several times higher on IL-17RB$^+$ NKT cells than on the other subsets, whereas no significant differences were found in *CXCR6* expression (Fig. 1 D), which is important for NKT cell migration (18). The results are consistent with the previous findings that NKT cells require CCR4 to localize to the airways and to induce AHR (19).

Concerning cytokine production of IL-17RB$^+$ NKT cells, it is reported that NKT cells produce both Th1 and Th2 cytokines at the same time upon stimulation with their ligand, α-GalCer (20). Surprisingly, IL-17RB$^+$ NKT cells expressed lower levels of Th1-related transcripts, such as *IFN-γ*, *T-bet*, *Stat4*, *IL-18Rβ*, and *IL-12Rβ2* (Fig. 1 E), whereas higher levels of the Th2-related transcript *IL-4* were detected (Fig. 1 F). In contrast, transcripts for cytotoxic effector molecules, such as *Granzyme*, *Perforin*, and *killer receptors* (*KIRa1*, *KIRc1*, *KIRd1*, and *KIRg1*), were expressed mainly in DN NKT cells (Fig. 1 G), supporting the previous findings that DN NKT but not $CD4^+$ NKT cells predominantly mediate antitumor immunity (19) and also that NKG2D was predominantly expressed on DN NKT cells, as shown in Fig. 1 C. The expression levels of *IL-17A* and *RORγt* transcripts in IL-17RB$^+$ NKT cells, which are high in Th17 cells, were lower than those in DN NKT cells (Fig. 1 H). These results on surface phenotypes and mRNA expression profiles clearly indicate that IL-17RB$^+$ NKT cells are Th2-type NKT cells and are distinct from other NKT cells, such as DN NKT cells or IL-17–producing NKT cells.

Next, we analyzed the function of IL-17RB$^+$ NKT cells in response to IL-25 in vitro. IL-17RB$^+$ NKT but not $CD4^+$ IL-17RB$^-$ nor DN NKT cells responded to IL-25 in a dose-dependent manner only in the presence of APCs (Fig. 2 A), which is similar to previous findings on the requirement of two signals, such as IL-12 and CD1d on APCs for IFN-γ production (21) and for IL-21 production (22), in NKT cell activation. Under these conditions, IL-25–activated IL-17RB$^+$ NKT cells mainly produced IL-13, along with modest production of IL-4, but barely produced IFN-γ (Fig. 2 B). Moreover, IL-17RB$^+$ NKT cells produced Th2 chemokines such as thymus and activation-regulated chemokine/CCL17, macrophage-derived chemokine/CCL22, and C10/CCL6 as well as eosinophil chemotactic factor–L (ECF-L) upon stimulation with IL-25 (Fig. 2 C). These results indicate that IL-25 triggers IL-17RB$^+$ NKT cells to preferentially produce the IL-13, Th2 chemokines, and ECF-L important for recruitment of eosinophils.

Recently, other IL-17 family members, IL-17A or IL-17F, have been shown to be involved in chronic inflammatory and allergic lung diseases (23, 24). The expression levels of *IL-17A* mRNA in IL-17RB$^+$ NKT cells were slightly elevated after treatment with IL-25 (Fig. 2 C). However, levels of *IL-17A* and *RORγt* mRNA in IL-17RB$^+$ NKT cells were lower than those in DN NKT cells (Fig. 1 H). Because high expression of *RORγt* is one of the markers for Th17 cells, low expression of *RORγt* in IL-17RB$^+$ NKT cells (Fig. 1 H) indicates that IL-17RB$^+$ NKT cells are distinct from IL-17–producing NKT cells. In addition, even though NK1.1-negative NKT cells represent IL-17–producing cells in C57BL/6 mice (25, 26), it

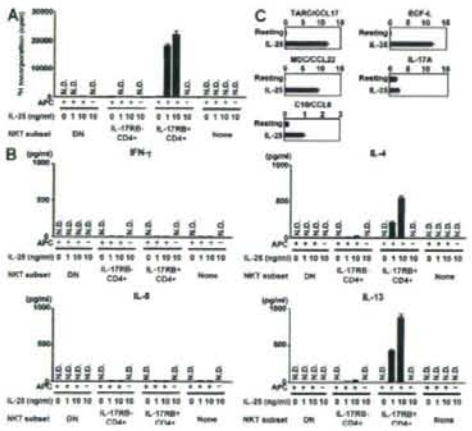

Figure 2. Properties of splenic IL-17RB$^+$ $CD4^+$ NKT cells. (A and B) Proliferation (A) and cytokine production (B) of DN, IL-17RB$^-$ $CD4^+$, and IL-17RB$^+$ $CD4^+$ NKT cells. Indicated NKT cell subpopulations (10^6 cells/ml) were co-cultured for 3 d with or without splenic $CD11c^+$ DCs (10^5 cells/ml) in the absence or presence of IL-25 (0, 1, and 10 ng/ml), and proliferation was assayed by [^{3}H]thymidine incorporation (A) or cytokine production by cytokine bead array (B). The data are shown as the means ± SD of three cultures. The data are representative of four independent experiments. (C) Quantitative analysis of genes in IL-17RB$^+$ $CD4^+$ NKT cells. IL-17RB$^+$ $CD4^+$ NKT cells (10^6 cells/ml) were co-cultured with splenic $CD11c^+$ DCs (10^5 cells/ml) in the presence of 10 ng/ml IL-25 for 48 h. IL-17RB$^+$ $CD4^+$ NKT cells were sorted and analyzed for their gene expression by quantitative real-time PCR, as described in Materials and methods. The data are representative of three independent experiments (means ± SEM).

Published November 17, 2008

has also been reported that IL-17–producing NKT cells are not restricted to a particular NKT cell subset (27). Another report has also revealed that ozone- but not allergen-induced AHR requires IL-17A produced from both NKT and T cells (28). These results suggest that IL-17RB$^+$ NKT cells described in this report are not equivalent to IL-17A–producing NKT cells reported by others.

We further examined whether the frequency of IL-17RB$^+$ NKT cells differs among mouse strains because allergic responses are strain dependent. Intriguingly, IL-17RB$^+$ NKT cells were fairly abundant in Th2-prone BALB/c and DBA2/cr mice but were barely detectable in Th1-prone C57BL/6 and C3H/HeN mice (Fig. S5, available at http://www.jem.org/cgi/content/full/jem.20080698/DC1). We also found that IL-17RB$^+$ NKT cells were detected more in the lung and spleen than the thymus but were almost undetectable in the liver. Although the number of NKT cells in the lung was one tenth of that in the spleen or the thymus, IL-17RB$^+$ NKT cells make up a higher proportion in the total NKT cells in the lung (Fig. 3 A). Similar to the splenic NKT cells shown in Fig. 1 A, the selective expression of IL-17RB on NKT cells was also detected in the lung, whereas conventional CD4$^+$ T, $\gamma\delta^+$ T, c-kit$^+$ NBNT, and noninvariant NKT cells in the lung were negative or barely detectable (Fig. 3 B).

To determine whether IL-17RB$^+$ NKT cells are required for IL-25 in the development of AHR, WT mice were

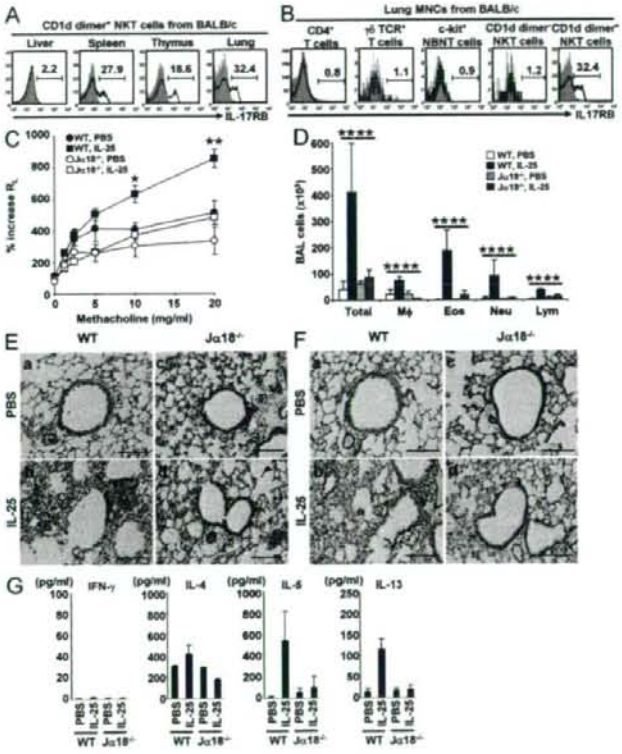

Figure 3. Involvement of IL-17RB$^+$ NKT cells in the development of IL-25–induced AHR. (A and B) Tissue distribution of IL-17RB$^+$ NKT cells (A) and IL-17RB expression among lung mononuclear cell populations (B) in BALB/c mice. α-GalCer/CD1d dimer$^+$ NKT cells in the indicated organs (A) and mononuclear cell populations in the lung (B) from BALB/c mice were gated and analyzed by FACS using B5F6 F(ab')$_2$ IL-17RB mAb. Shaded profiles in the histograms indicate the background staining with rat F(ab')$_2$ IgG2a ($n = 3$). Percentages are shown. (C) Development of AHR. The changes in R_L were measured. The detailed method for development of OVA/IL-25–induced AHR is described in Materials and methods. Results are expressed as the mean ± SEM. The group of IL-25–treated WT mice was compared with three other groups. *, $P < 0.05$; and **, $P < 0.01$ calculated by ANOVA. The results represent one out of three experiments with five mice in each group. (D and G) Total and differential cell counts (D) and cytokines (G) in BAL fluid. BAL fluid was collected 24 h after challenge with intranasal OVA of the mice depicted in C. IL-25–induced pulmonary inflammation (D) and IL-13 and IL-5 production (G) were reduced in Jα18$^{-/-}$ mice. The data on cytokines in G are expressed as the amounts detected in the 10-fold PBS-diluted BAL samples. Results are expressed as means ± SEM. *, $P < 0.05$; **, $P < 0.01$. The group of IL-25–treated WT mice was compared with three other groups. These results represent one out of four experiments with five mice in each group. (E and F) Histological analysis of lung tissues with hematoxylin and eosin (E) and periodic acid Schiff (F) staining. IL-25–treated WT (c) or Jα18$^{-/-}$ (d) mice were compared with WT (a) or Jα18$^{-/-}$ (b) mice from control ($n = 4$). Bars, 100 μm.

Published November 17, 2008

immunized with a suboptimal dose of OVA/alum twice and were subsequently treated with PBS before a single intranasal OVA challenge (see Materials and methods). Under these conditions, the mice failed to develop AHR. When the mice were subsequently treated with IL-25 instead of PBS, they developed AHR (Fig. 3 C). In contrast, even after treatment with IL-25, NKT cell–deficient $J\alpha18^{-/-}$ mice failed to develop significant AHR, comparable to that seen in the PBS-treated control mice (Fig. 3 C). Unlike WT mice, $J\alpha18^{-/-}$ mice treated with IL-25 significantly reduced numbers of airway macrophages, eosinophils, neutrophils, and lymphocytes in the lung (Fig. 3 D).

Hematoxylin and eosin staining of the lung tissue of IL-25–treated WT mice revealed that the levels of infiltration of inflammatory mononuclear cells into the peribronchiolar region were higher in WT mice with severe tissue destruction compared with those in $J\alpha18^{-/-}$ mice. No inflammatory cell infiltration was detected in untreated WT or $J\alpha18^{-/-}$ mice (Fig. 3 E). By periodic acid Schiff staining, mucus-producing cells were abundant only in IL-25–treated WT but not $J\alpha18^{-/-}$ mice (Fig. 3 F). To further investigate the effects on allergic responses mediated by IL-17RB$^+$ NKT cells, we examined cytokine production in the bronchoalveolar lavage (BAL) fluid of IL-25–treated WT or $J\alpha18^{-/-}$ mice and controls. The production of IL-5 and IL-13, which plays a crucial role in the recruitment of eosinophils and Th2 cells, respectively, were detected only in IL-25–treated WT mice (Fig. 3 G). Even though IL-17RB$^+$ NKT cells did not produce IL-5 upon IL-25 stimulation (Fig. 2 B), they produced ECF-L (Fig. 2 C), which is important for the recruitment of eosinophils producing IL-5. These results strongly suggest that IL-25 acts directly on NKT cells and induces AHR.

We then investigated whether IL-17RB$^+$ NKT cells are involved in the development of IL-25–dependent AHR, and we depleted IL-17RB$^+$ cells with 3H8 IL-17RB mAb. Among the NKT cell populations, the majority of IL-17RB$^+$ NKT cells were α-GalCer/CD1d dimer^{hi} TCRβ^{hi}, indicating that the expression level of TCRα and TCRβ on IL-17RB$^+$ NKT cells was higher than that on other IL-17RB$^-$ NKT cells (Fig. 4 A). IL-17RB$^+$ NKT depletion persisted for at least 5 d after 3H8 IL-17RB mAb injection (Fig. 4 B), whereas no effects were detected on other cell types, such as CD4$^+$ T, γδ$^+$ T, and NBNT c-kit$^+$ cells (Fig. S6, available at http://www.jem.org/cgi/content/full/jem.20080698/DC1). As expected, treatment of 3H8 IL-17RB mAb significantly induced suppression of AHR (Fig. 4 C), which was tightly correlated with the reduction of the number of IL-17RB$^+$ NKT cells (Fig. 4 B). Administration of an isotype-matched control mAb did not suppress AHR (Fig. 4 C), and the number of IL-17RB$^+$ NKT cells remained unchanged (Fig. 4 B).

To confirm the findings that IL-17RB$^+$ NKT cells are essential for the development of IL-25–dependent AHR, we transferred enriched splenic IL-17RB$^+$ NKT cells into $J\alpha18^{-/-}$ mice and tested their ability to develop IL-25–dependent AHR (Fig. 4 D). The cell transfer of IL-17RB$^+$ NKT cells, but not IL-17RB$^-$ NKT cells nor PBS alone, restored AHR induced by OVA plus IL-25, indicating that IL-17RB$^+$ NKT cells in the lung are functionally equivalent to those in the spleen. In addition, when equal numbers of cells were transferred, the severity of AHR induced by enriched IL-17RB$^+$ NKT cells was almost three times higher than the total spleen NKT cells (Fig. 4 D), consistent with the ratio of IL-17RB$^+$ NKT cells (Fig. 1 B). This indicates that the severity of AHR depends on the cell numbers of IL-17RB$^+$ NKT cells transferred (Fig. 4 D) and, thus, that IL-17RB$^+$ NKT cells contribute to the development of IL-25–dependent AHR.

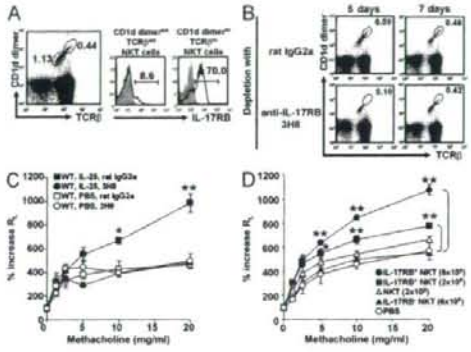

Figure 4. Requirement of IL-17RB$^+$ NKT cells in the development of IL-25–induced AHR. (A) FACS profiles of NKT cells in the expression of IL-17RB. α-GalCer/CD1d dimer^{hi} TCRβ^{hi} NKT cells and α-GalCer/CD1d dimer^{int} TCRβ^{int} NKT cells in the spleen from BALB/c mice were gated, and IL-17RB expression was analyzed using F(ab')$_2$ IL-17RB mAb B5F6. IL-17RB was preferentially expressed in α-GalCer/CD1d dimer^{hi} TCRβ^{hi} NKT cells ($n = 3$). (B) FACS profiles of NKT cells in mice treated with IL-17RB mAb. α-GalCer/CD1d dimer$^+$ TCRβ$^+$ NKT cells in the spleen from BALB/c mice at the indicated days after injection of 3H8 IL-17RB mAb or control rat IgG2a (1 mg/mouse) were gated and analyzed by FACS. Depletion of IL-17RB$^+$ NKT cells persisted for at least 5 d after 3H8 injection because of the absence of α-GalCer/CD1d dimer^{hi} TCRβ^{hi} NKT cells in A ($n = 2$). Percentages are shown. (C) Development of AHR in mice treated with IL-17RB mAb. The detailed method for development of OVA/IL-25–induced AHR is described in Materials and methods. In brief, OVA/alum-sensitized mice were injected with 3H8 IL-17RB mAb or rat IgG2a (1 mg/mouse) 24 h before 2 μg IL-25 or PBS treatment and were challenged with OVA after 24 h, and R_L was determined after 48 h. The group of rat IgG2a–treated WT mice was compared with three other groups. Results are expressed as means ± SEM. The results represent one out of three experiments with five mice in each group. *, $P < 0.05$; and **, $P < 0.01$ calculated by ANOVA. (D) AHR development after cell transfer of spleen IL-17RB$^+$ NKT cells into $J\alpha18^{-/-}$ mice. The detailed method for development of OVA/IL-25–induced AHR is described in Materials and methods. Indicated cell numbers of sorted IL-17RB$^+$, IL-17RB$^-$ NKT, or total NKT cells from spleen or PBS control were intravenously transferred into OVA/alum-sensitized $J\alpha18^{-/-}$ mice 24 h before treatment with 3 μg IL-25 and were challenged with OVA after 24 h, and R_L was measured after 48 h. Each group of IL-17RB$^+$ NKT cell–transferred mice was compared with three other groups. *, $P < 0.05$; and **, $P < 0.01$ calculated by the Kruskal-Wallis test. The results represent one out of four experiments with five mice in each group. Results are expressed as means ± SEM.

Published November 17, 2008

Although we have not identified the cells producing IL-25 in the present report, it is detected in lung biopsy samples from patients with asthma (29). In addition, IL-25 has been reported to induce inflammatory cytokine and chemokine production by human lung fibroblasts, and components of extracellular matrix by airway smooth muscle cells (29). These reports have also suggested that IL-25 plays a role in human asthma (29). Our findings clearly revealed IL-17RB$^+$ NKT cells as target cells of IL-25 in the development of AHR or asthma. The efficacy with which IL-17RB antibodies prevent AHR and reduce Th2-cytokine–induced inflammation in vivo suggests that IL-17RB is an ideal therapeutic target for asthma.

MATERIALS AND METHODS

Mice. BALB/c mice were purchased from Charles River Laboratories or Clea Japan, Inc. Jα18-deficient mice were generated as previously described (30) and were backcrossed >10 times to BALB/c mice. Mice were kept under specific pathogen-free conditions and were used at 8–16 wk of age. All experiments were in accordance with protocols approved by the RIKEN Animal Care and Use Committee.

Generation of mouse IL-17RB–specific mAbs. The IL-17RB–Ig fusion gene was created by fusing the cDNA of the extracellular domain of mouse IL-17RB in frame to the CH2/CH3 domains of human IgG1 in the pIRES2-EGFP expression vector (Clontech Laboratories, Inc.). IL-17RB–Ig was purified from the culture supernatants of transfected HEK293 cells using a protein A–sepharose column (GE Healthcare; Fig. S2). Mouse IL-17RB mAbs were produced by immunizing Wister rats with IL-17RB–Ig. After initial screening by ELISA on IL-17RB–Ig fusion protein, 100 hybridoma clones were further characterized by flow cytometry on IL-17RB transfectants (Fig. S1).

OVA/IL-25–induced AHR model. The original protocol for induction of AHR by OVA sensitization (100 μg three times) and challenge (100 μg OVA/alum three times), as previously described (16), was modified in the present study. In our modified method, mice were intraperitoneally immunized with a suboptimal dose of OVA/alum twice and were subsequently challenged once with intranasal OVA at the same time points as described. In this model, BALB/c mice failed to induce development of AHR, cell infiltration, and histological changes in the lung without IL-25 but induced AHR with intravenous injection of IL-25 (Fig. 3). In brief, mice were intraperitoneally immunized with 50 μg/2 mg OVA/alum twice at a 1-wk interval. 7 d later, mice were treated intravenously with 2 μg/200 μl IL-25 or 200 μl of control PBS at 2 d before intranasal challenge with 50 μg OVA. 24 h later, AHR responses were measured. For transfer of IL-17RB$^+$, IL-17RB$^-$ NKT, or total NKT cells, cells were sorted by a FACSAria (BD). Sorted cells or PBS alone were intravenously injected 1 d before IL-25 treatment (Fig. 4 D). For depletion of IL-17RB$^+$ cells, 1 mg 3H8 IL-17RB mAb was intraperitoneally injected 5 d before AHR measurement (Fig. 4 C).

Measurement of airway responsiveness. Airway function was measured for changes in lung resistance (R_L) and dynamic compliance in response to increasing doses of inhaled methacholine (1.25, 2.5, 5, 10, and 20 mg/ml) by using an invasive flexiVent (SCIREQ Scientific Respiratory Equipment Inc.).

Lymphocyte isolation and analysis of BAL fluid. After measurement of AHR and death, the lung of the mouse trachea canulated was lavaged twice with 1 ml PBS (~10-fold PBS dilution), and the BAL fluid was pooled as previously described (13). Spleen, blood, and lung lymphocytes were isolated as described previously (31).

Cytokine measurement. BAL fluid and culture supernatants were collected and analyzed by cytometric bead array (BD) according to the manufacturer's protocol.

Flow cytometry. Antibodies used for flow cytometric analysis were as follows: FITC anti-mouse TCRβ (H57-597; BD), Pacific blue anti-mouse CD4 (RM4-5; BD), PerCP-Cy5.5 anti-mouse CD8α (53-6.7; BD), PE anti-mouse CD44 (IM7; BD), PE anti-mouse CD122 (TM-β1; BD), PE anti-mouse CD62L (MEL-14; BD), and PE anti-mouse NKG2D (C7; eBioscience).

Proliferation assay. Proliferation assays were done in 96-well U-bottomed plates. The spleen cell cultures were incubated for 3 d and pulsed with 0.037 MBq/well of [^{3}H]thymidine (GE Healthcare) for the last 16 h. Radioactivity was measured using a MicroBeta (PerkinElmer).

Quantitative real-time PCR. The PCR was performed with the Platinum SYBR Green qPCR SuperMix-UGD kit with ROX (Invitrogen) according to the protocol provided. A sequence detection system (ABI PRISM 7900HT; Applied Biosystems) was used for quantitative real-time PCR according to the manufacturer's instructions. To ensure the specificity of the amplification products, a melting curve analysis was performed. Results were normalized using the internal control gene HPRT. Sequences of PCR primers (Table S1) were designed with Primer Express software (Applied Biosystems) for optimal product length, germinal center content, and Tm value.

Statistical analysis. The statistical significance of differences was determined by analysis of variance (ANOVA) or the Kruskal-Wallis test. The values were expressed as means ± SEM from independent experiments. Any difference with a p-value of <0.05 was considered significant (*, $P < 0.05$; **, $P < 0.01$).

Online supplemental material. Fig. S1 shows generation of mouse IL-17RB–specific mAbs. Fig. S2 shows expression and purification of mouse IL-17RB–Ig fusion protein. Fig. S3 shows FACS profiles of cells stained with mouse IL-17RB–specific mAbs. Fig. S4 shows RT-PCR analysis on c-kit$^+$ NBNT cells and NKT cell subsets. Fig. S5 provides IL-17RB$^+$ NKT cells in different mouse strains. Fig. S6 shows FACS analysis on CD4$^+$ T, γδ$^+$ T, and c-kit$^+$ NBNT cells in mice treated with anti–IL-17RB mAb. Table S1 lists primers used for quantitative real-time PCR analysis. Online supplemental material is available at http://www.jem.org/cgi/content/full/jem.20080698/DC1.

We thank P.D. Burrows for critical reading; S. Seki, T. Aoyama, A. Hijikata, and H. Kitamura for technical assistance; T. Tashiro and K. Mori for α-GalCer synthesis; and N. Takeuchi for secretarial assistance.

The authors have no conflicting financial interests.

Submitted: 2 April 2008
Accepted: 23 October 2008

REFERENCES

1. Umetsu, D.T., and R.H. DeKruyff. 2006. The regulation of allergy and asthma. *Immunol. Rev.* 212:238–255.
2. Fallon, P.G., H.E. Jolin, P. Smith, C.L. Emson, M.J. Townsend, R. Fallon, P. Smith, and A.N. McKenzie. 2002. IL-4 induces characteristic Th2 responses even in the combined absence of IL-5, IL-9, and IL-13. *Immunity.* 17:7–17.
3. Wills-Karp, M. 1999. Immunological basis of antigen-induced airway hyperresponsiveness. *Annu. Rev. Immunol.* 17:255–281.
4. Wills-Karp, M., J. Luyimbazi, X. Xu, B. Schofield, T.Y. Neben, C.L. Karp, and D.D. Donaldson. 1998. Interleukin-13: central mediator of allergic asthma. *Science.* 282:2258–2261.
5. Fort, M.M., J. Cheung, D. Yen, J. Li, S.M. Zurawski, S. Lo, S. Menon, T. Clifford, B. Hunte, R. Lesley, et al. 2001. IL-25 induces IL-4, IL-5, and IL-13 and Th2-associated pathologies in vivo. *Immunity.* 15:985–995.
6. Pan, G., D. French, W. Mao, M. Maruoka, P. Risser, J. Lee, J. Foster, S. Aggarwal, K. Nicholes, S. Guillet, et al. 2001. Forced expression of murine IL-17E induces growth retardation, jaundice, a Th2-biased response, and multiorgan inflammation in mice. *J. Immunol.* 167:6559–6567.
7. Kim, M.R., R. Manoukian, R. Yeh, S.M. Silbiger, D.M. Danilenko, S. Scully, J. Sun, M.L. DeRose, M. Stolina, D. Chang, et al. 2002.

Published November 17, 2008

Transgenic overexpression of human IL-17E results in eosinophilia, B-lymphocyte hyperplasia, and altered antibody production. *Blood*. 100:2330–2340.

8. Ikeda, K., H. Nakajima, K. Suzuki, S. Kagami, K. Hirose, A. Suto, Y. Saito, and I. Iwamoto. 2003. Mast cells produce interleukin-25 upon Fc epsilon RI-mediated activation. *Blood*. 101:3594–3596.
9. Tamachi, T., Y. Maezawa, K. Ikeda, S. Kagami, M. Hatano, Y. Seto, A. Suto, K. Suzuki, N. Watanabe, Y. Saito, et al. 2006. IL-25 enhances allergic airway inflammation by amplifying a TH2 cell-dependent pathway in mice. *J. Allergy Clin. Immunol*. 118:606–614.
10. Hurst, S.D., T. Muchamuel, D.M. Gorman, J.M. Gilbert, T. Clifford, S. Kwan, S. Menon, B. Seymour, C. Jackson, T.T. Kung, et al. 2002. New IL-17 family members promote Th1 or Th2 responses in the lung: in vivo function of the novel cytokine IL-25. *J. Immunol*. 169:443–453.
11. Ballantyne, S.J., J.L. Barlow, H.E. Jolin, P. Nath, A.S. Williams, K.F. Chung, G. Sturton, S.H. Wong, and A.N. McKenzie. 2007. Blocking IL-25 prevents airway hyperresponsiveness in allergic asthma. *J. Allergy Clin. Immunol*. 120:1324–1331.
12. Fallon, P.G., S.J. Ballantyne, N.E. Mangan, J.L. Barlow, A. Dasvarma, D.R. Hewett, A. McIlgorm, H.E. Jolin, and A.N. McKenzie. 2006. Identification of an interleukin (IL)-25–dependent cell population that provides IL-4, IL-5, and IL-13 at the onset of helminth expulsion. *J. Exp. Med*. 203:1105–1116.
13. Akbari, O., P. Stock, E. Meyer, M. Kronenberg, S. Sidobre, T. Nakayama, M. Taniguchi, M.J. Grusby, R.H. DeKruyff, and D.T. Umetsu. 2003. Essential role of NKT cells producing IL-4 and IL-13 in the development of allergen-induced airway hyperreactivity. *Nat. Med*. 9:582–588.
14. Meyer, E.H., S. Goya, O. Akbari, G.J. Berry, P.B. Savage, M. Kronenberg, T. Nakayama, R.H. DeKruyff, and D.T. Umetsu. 2006. Glycolipid activation of invariant T cell receptor+ NK T cells is sufficient to induce airway hyperreactivity independent of conventional CD4+ T cells. *Proc. Natl. Acad. Sci. USA*. 103:2782–2787.
15. Moseley, T.A., D.R. Haudenschild, L. Rose, and A.H. Reddi. 2003. Interleukin-17 family and IL-17 receptors. *Cytokine Growth Factor Rev*. 14:155–174.
16. Crowe, N.Y., J.M. Coquet, S.P. Berzins, K. Kyparissoudis, R. Keating, D.G. Pellicci, Y. Hayakawa, D.I. Godfrey, and M.J. Smyth. 2005. Differential antitumor immunity mediated by NKT cell subsets in vivo. *J. Exp. Med*. 202:1279–1288.
17. Jamieson, A.M., A. Diefenbach, C.W. McMahon, N. Xiong, J.R. Carlyle, and D.H. Raulet. 2002. The role of the NKG2D immunoreceptor in immune cell activation and natural killing. *Immunity*. 17:19–29.
18. Johnston, B., C.H. Kim, D. Soler, M. Emoto, and E.C. Butcher. 2003. Differential chemokine responses and homing patterns of murine TCR alpha beta NKT cell subsets. *J. Immunol*. 171:2960–2969.
19. Meyer, E.H., M.A. Wurbel, T.L. Staton, M. Pichavant, M.J. Kan, P.B. Savage, R.H. DeKruyff, E.C. Butcher, J.J. Campbell, and D.T. Umetsu. 2007. iNKT cells require CCR4 to localize to the airways and to induce airway hyperreactivity. *J. Immunol*. 179:4661–4671.
20. Taniguchi, M., M. Harada, S. Kojo, T. Nakayama, and H. Wakao. 2003. The regulatory role of Valpha14 NKT cells in innate and acquired immune response. *Annu. Rev. Immunol*. 21:483–513.
21. Brigl, M., L. Bry, S.C. Kent, J.E. Gumperz, and M.B. Brenner. 2003. Mechanism of CD1d-restricted natural killer T cell activation during microbial infection. *Nat. Immunol*. 4:1230–1237.
22. Harada, M., K. Magara-Koyanagi, H. Watarai, Y. Nagata, Y. Ishii, S. Kojo, S. Horiguchi, Y. Okamoto, T. Nakayama, N. Suzuki, et al. 2006. IL-21–induced Bε cell apoptosis mediated by natural killer T cells suppresses IgE responses. *J. Exp. Med*. 203:2929–2937.
23. Rahman, M.S., A. Yamasaki, J. Yang, L. Shan, A.J. Halayko, and A.S. Gounni. 2006. IL-17A induces eotaxin-1/CC chemokine ligand 11 expression in human airway smooth muscle cells: role of MAPK (Erk1/2, JNK, and p38) pathways. *J. Immunol*. 177:4064–4071.
24. Hizawa, N., M. Kawaguchi, S.K. Huang, and M. Nishimura. 2006. Role of interleukin-17F in chronic inflammatory and allergic lung disease. *Clin. Exp. Allergy*. 36:1109–1114.
25. Michel, M.L., A.C. Keller, C. Paget, M. Fujio, F. Trottein, P.B. Savage, C.H. Wong, E. Schneider, M. Dy, and M.C. Leite-de-Moraes. 2007. Identification of an IL-17–producing NK1.1neg iNKT cell population involved in airway neutrophilia. *J. Exp. Med*. 204:995–1001.
26. Coquet, J.M., S. Chakravarti, K. Kyparissoudis, F.W. McNab, L.A. Pitt, B.S. McKenzie, S.P. Berzins, M.J. Smyth, and D.I. Godfrey. 2008. Diverse cytokine production by NKT cell subsets and identification of an IL-17–producing CD4−NK1.1− NKT cell population. *Proc. Natl. Acad. Sci. USA*. 105:11287–11292.
27. Rachitskaya, A.V., A.M. Hansen, R. Horai, Z. Li, R. Villasmil, D. Luger, R.B. Nussenblatt, and R.R. Caspi. 2008. Cutting edge: NKT cells constitutively express IL-23 receptor and RORgammat and rapidly produce IL-17 upon receptor ligation in an IL-6-independent fashion. *J. Immunol*. 180:5167–5171.
28. Pichavant, M., S. Goya, E.H. Meyer, R.A. Johnston, H.Y. Kim, P. Matangkasombut, M. Zhu, Y. Iwakura, P.B. Savage, R.H. DeKruyff, et al. 2008. Ozone exposure in a mouse model induces airway hyperreactivity that requires the presence of natural killer T cells and IL-17. *J. Exp. Med*. 205:385–393.
29. Létuvé, S., S. Lajoie-Kadoch, S. Audusseau, M.E. Rothenberg, P.O. Fiset, M.S. Ludwig, and Q. Hamid. 2006. IL-17E upregulates the expression of proinflammatory cytokines in lung fibroblasts. *J. Allergy Clin. Immunol*. 117:590–596.
30. Cui, J., T. Shin, T. Kawano, H. Sato, E. Kondo, I. Toura, Y. Kaneko, H. Koseki, M. Kanno, and M. Taniguchi. 1997. Requirement for Vα14 NKT cells in IL-12-mediated rejection of tumors. *Science*. 278:1623–1626.
31. Watarai, H., R. Nakagawa, M. Omori-Miyake, N. Dashtsoodol, and M. Taniguchi. 2008. Methods for detection, isolation and culture of mouse and human invariant NKT cells. *Nat. Protoc*. 3:70–78.

Published May 12, 2008

JEM

ARTICLE

Development and characterization of IL-21–producing CD4+ T cells

Akira Suto,[1,2] Daisuke Kashiwakuma,[2] Shin-ichiro Kagami,[1,2] Koichi Hirose,[2] Norihiko Watanabe,[2] Kotaro Yokote,[3] Yasushi Saito,[3] Toshinori Nakayama,[4] Michael J. Grusby,[5] Itsuo Iwamoto,[6] and Hiroshi Nakajima[1,2]

[1]Department of Molecular Genetics, Graduate School of Medicine, [2]Department of Allergy and Clinical Immunology, Chiba University Hospital, [3]Department of Clinical Cell Biology, and [4]Department of Immunology, Graduate School of Medicine, Chiba University, Chiba, 260-8670 Japan
[5]Department of Immunology and Infectious Diseases, Harvard School of Public Health, Boston, MA 02115
[6]Research Center for Allergy and Clinical Immunology, Asahi General Hospital, Asahi, Chiba, 289-2511 Japan

It has recently been shown that interleukin (IL)-21 is produced by Th17 cells, functions as an autocrine growth factor for Th17 cells, and plays critical roles in autoimmune diseases. In this study, we investigated the differentiation and characteristics of IL-21–producing CD4+ T cells by intracellular staining. Unexpectedly, we found that under Th17-polarizing conditions, the majority of IL-21–producing CD4+ T cells did not produce IL-17A and -17F. We also found that IL-6 and -21 potently induced the development of IL-21–producing CD4+ T cells without the induction of IL-4, IFN-γ, IL-17A, or IL-17F production. On the other hand, TGF-β inhibited IL-6– and IL-21–induced development of IL-21–producing CD4+ T cells. IL-2 enhanced the development of IL-21–producing CD4+ T cells under Th17-polarizing conditions. Finally, IL-21–producing CD4+ T cells exhibited a stable phenotype of IL-21 production in the presence of IL-6, but retained the potential to produce IL-4 under Th2-polarizing conditions and IL-17A under Th17-polarizing conditions. These results suggest that IL-21–producing CD4+ T cells exhibit distinct characteristics from Th17 cells and develop preferentially in an IL-6–rich environment devoid of TGF-β, and that IL-21 functions as an autocrine growth factor for IL-21–producing CD4+ T cells.

CORRESPONDENCE
Hiroshi Nakajima:
nakajimh@faculty.chiba-u.jp

Activated CD4+ T cells differentiate into at least three distinct effector subsets as defined by their patterns of cytokine production (1–4). Th1 cells produce IFN-γ and lymphotoxin and play a critical role in protective immunity against intracellular pathogens (1–4). Th2 cells produce IL-4, -5, and -13 and are essential for the expulsion of parasites (1–4). Newly identified Th17 cells produce IL-17A and -17F and play a pathogenic role in a variety of autoimmune diseases (1–5). Recently, it has been reported that IL-21 is another cytokine highly produced by Th17 cells and that it promotes the development of Th17 cells (6–9).

IL-21 is a four-helix-bundle type I cytokine with significant homology to IL-2, -15, and -4 (10–12). IL-21 has been demonstrated to be expressed in Th2 cells (13), follicular B helper T cells (14), and NK T cells (15) and to exhibit pleiotropic effects on the proliferation, differentiation, and effector function of T, B, NK, and dendritic cells (10–12). In vivo, it has been shown that IL-21 is involved in several autoimmune disease models. For example, lymphopenia and compensatory IL-21–mediated homeostatic expansion of lymphocytes has been reported to be involved in the development of autoimmunity in NOD mice (16). The excessive production of IL-21 has been shown to be associated with the development of high titers of autoantibodies and a lupus-like pathology in *Sanroque* mice (17). Furthermore, a blockade of IL-21 signaling has been demonstrated to ameliorate mouse models of rheumatoid arthritis and lupus (18, 19). However, the characteristic of IL-21–producing CD4+ T cells, especially in their relation to Th17 cells, is still unknown because a single-cell analysis of IL-21–producing cells has not been achieved yet.

A. Suto and D. Kashiwakuma contributed equally to this work.

J. Exp. Med. Vol. 205 No. 6 1369-1379 www.jem.org/cgi/doi/10.1084/jem.20072057

Published May 12, 2008

In this study, by establishing the intracellular staining of IL-21, we found that although IL-21–producing CD4+ T cells developed preferentially under Th17-polarizing conditions, a considerable number of IL-21–producing CD4+ T cells were negative for intracellular IL-17A and -17F. We also found that IL-6 potently induced the development of IL-21–producing CD4+ T cells without the induction of IL-4, IFN-γ, IL-17A, or IL-17F production. On the other hand, TGF-β inhibited the IL-6–induced development of IL-21–producing CD4+ T cells. In addition, IL-2 significantly enhanced the development of IL-21–producing CD4+ T cells under Th17-polarizing conditions. IL-21 itself also induced the development of IL-21–producing CD4+ T cells. IL-21–producing CD4+ T cells exhibited a stable phenotype of IL-21 production in the presence of IL-6, but still had a potential to produce IL-4 under Th2-polarizing conditions and IL-17A under Th17-polarizing conditions. Our results suggest that IL-21–producing CD4+ T cells exhibit distinct characteristics from Th17 cells, that IL-21–producing CD4+ T cells develop preferentially in an IL-6–rich environment devoid of TGF-β, and that IL-21 functions as an autocrine growth factor for IL-21–producing CD4+ T cells.

RESULTS

IL-21–producing CD4+ T cells develop preferentially under Th17-polarizing conditions, but the majority of them are negative for intracellular IL-17A and -17F

Recently, it has been shown that Th17 cells produce a large amount of IL-21 compared with Th2 and Th1 cells, and that IL-21 functions as an autocrine growth factor for Th17 cells (6–9). We also found that IL-21 was produced by activated CD4+ T cells under Th17-polarizing conditions (in the presence of IL-6, TGF-β, anti–IL-4 mAb, and anti–IFN-γ mAb) much greater than under Th2-polarizing conditions or under Th1-polarizing conditions (Fig. 1 A). However, it was still unclear whether IL-21 is actually produced by Th17 cells and what is the developmental and phenotypic characteristic of IL-21–producing CD4+ T cells because IL-21 production has not been determined at single-cell levels as yet. To address these issues, we established the intracellular cytokine staining of IL-21. We first generated several IL-21–producing Ba/F3 cell clones using a bicistronic retrovirus system and measured the levels of IL-21 in the culture supernatants by ELISA. Among these clones, Ba/F3-IL-21-GFP #6 cells produced a significant amount of IL-21 (Fig. 1 B, left), and we used this clone as a positive control for intracellular staining of IL-21. To detect intracellular IL-21, we used mouse IL-21R/human Fc-chimera (IL-21R-Fc) to capture IL-21 and anti-human Fc PE to visualize IL-21–IL-21R-Fc complexes. When cells were stained by this method, positive signals were detected in Ba/F3-IL-21-GFP #6 cells, but not in control Ba/F3-empty-GFP cells (Fig. 1 B, right). In the absence of IL-21R-Fc, no positive signal was detected (Fig. 1 B, right), confirming the correct detection of IL-21 by the intracellular staining.

By using the intracellular staining of IL-21, we examined IL-21–producing CD4+ T cells at single-cell levels. When

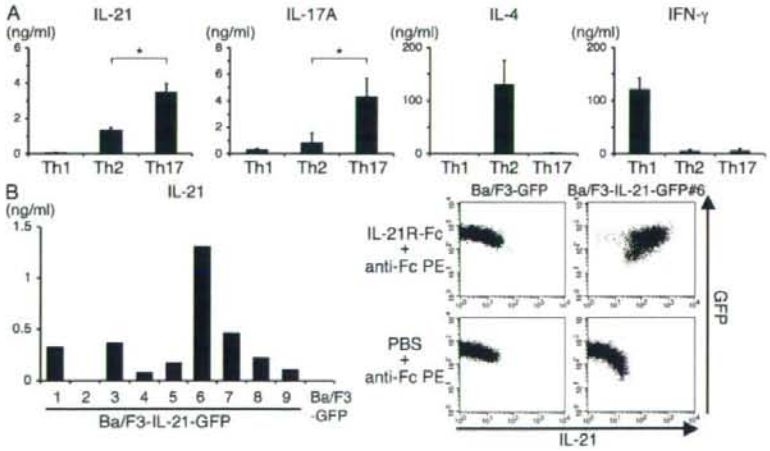

Figure 1. Establishment of a single-cell analysis of IL-21–producing cells. (A) IL-21 and -17A are produced by activated CD4+ T cells under Th17-polarizing conditions. Purified CD4+ T cells from lymph nodes of C57BL/6 mice were stimulated with anti-CD3 mAb/anti-CD28 mAb under Th1-, Th2-, and Th17-polarizing conditions. On day 5, 10^6 cells were restimulated with anti-CD3 mAb/anti-CD28 mAb for 24 h. The levels of cytokines in the culture supernatants were measured by ELISA. Data are the means ± the SD from four independent experiments. *, $P < 0.01$. (B) Establishment of a single-cell analysis of IL-21–producing cells. Ba/F3 cells were infected with pMX-IL-21-IRES-GFP retrovirus or control retrovirus (pMX-IRES-GFP). Nine clones of pMX-IL-21-IRES-GFP retrovirus-infected Ba/F3 cells (Ba/F3-IL-21-GFP cells) and one clone of control retrovirus-infected Ba/F3 cells (Ba/F3-GFP cells) were selected by limiting dilution. IL-21 in the culture supernatants was measured by ELISA (left). Ba/F3-GFP cells and Ba/F3-IL-21-GFP clone #6 cells were fixed, permeabilized, and incubated with IL-21R-Fc or PBS. After washing, cells were visualized with anti-Fc PE (right).